LOS ALAMOS SCIENTIFIC LABORATORY
of the
University of California
LOS ALAMOS • NEW MEXICO

MCNA: A Computer Program to Solve the Adjoint Neutron Transport Equation by Coupled Sampling with the Monte Carlo Method

by

Leland L. Carter

CONTENTS

MCNA: A COMPUTER PROGRAM TO SOLVE THE ADJOINT NEUTRON TRANSPORT EQUATION BY COUPLED SAMPLING WITH THE MONTE CARLO METHOD

by

Leland L. Carter

ABSTRACT

A coupled sampling technique that utilizes the Monte Carlo method of solution has been reported in the literature. This report extends this coupled sampling technique to include nuclear fission and time dependence. In the coupled sampling, specific use is made of sampling from the neutron transport equation to construct a scheme for a near-optimal subsequent sampling from the adjoint neutron transport equation. This procedure may be expected to be advantageous when the phase-space volume contributing to the functional is smaller than the phase-space volume of the neutron source.

The computer program MCNA was written to utilize the coupled sampling technique. MCNA uses the same neutron interaction models and cross-section library as does the Los Alamos code MCN; MCN solves the transport equation with Monte Carlo.

I. INTRODUCTION

The central limit theorem asserts that the average of n independent random variables (the sum of the random variables divided by n) has an approximately normal distribution when n is large;[1] this holds true under suitable mild conditions specified in the standard textbooks. Under the assumption of normality, a known probability may be assigned to the statement that "the theoretical expectation value lies within the band defined by the average value of the n independent observations $\pm\epsilon$." Here ϵ is proportional to the square root of the variance of the distribution. The variance of the distribution is proportional to the variance of an individual random variable and inversely proportional to n, and, hence, any given precision (ϵ/true value) may be obtained simply by taking enough random samples.

The fact that the precision decreases only inversely proportional to the square root of the number of samples may lead to an exorbitant amount of computation time for the required accuracy. If so,

an alternative method of reducing ϵ is to change the probability distributions used to obtain the random variables so that the theoretical variance of an individual sample is reduced.

Many problems of neutron transport cannot be solved efficiently with analog* Monte Carlo owing to the large theoretical variance of the individual samples. It is well known that certain advantages are realized in some of these problems through the solution of the corresponding adjoint equations. A commonly occurring example is the determination of a reaction rate in a small volume of phase space due to a given neutron source distribution. The variance in the estimate of the reaction rate for an individual neutron history is large because only a small fraction of the neutrons pass through the small phase-space volume of interest. Solution of the corresponding adjoint equation allows the sample histories to begin in the small phase-space volume.

---

*Analog refers to a direct simulation of neutron transport.

These histories are traced "backward" to the phase-space volume of the neutron source and contribute to the estimate of the reaction rate while in the phase-space volume of the source. The computation time required to obtain a given confidence limit in this adjoint solution depends upon the scheme utilized to sample from the adjoint equation.

The computer code MCNA is based upon a coupled sampling approach. Near-optimum density functions for sampling from the adjoint equation are obtained in this coupled sampling by approximating a theoretically feasible "zero-variance" scheme. The coupled sampling consists of sampling from the transport equation to construct the scheme for sampling from the adjoint equation, and then estimating the functional(s) by sampling from the adjoint equation.*

The coupled sampling approach discussed in Sec. II is an extension of Refs. 2 and 3 to include fission and time dependence. A brief description of the computer code MCNA is given in Sec. III. The physical models utilized and the geometry routine of the MCNA code are identical to those of the MCNA code;[4-6] MCN solves the neutron transport equation with Monte Carlo. The MCNA code is written in FORTRAN IV and is presently utilized on the CDC 6600 and CDC 7600 computers. An example problem is discussed in Sec. IV.

II. SAMPLING FROM THE ADJOINT TRANSPORT EQUATION AND COUPLED SAMPLING

A. General Discussion

The relevant equations may be derived by beginning with the Boltzmann integro-differential neutron transport equation,[7]

$$LG(\underline{R};\underline{R}') = \frac{1}{v}\frac{\partial G(\underline{R};\underline{R}')}{\partial t} + \underline{\Omega}\cdot\nabla G(\underline{R};\underline{R}') + \Sigma_t(\underline{R})G(\underline{R};\underline{R}')$$

$$- \int_{\underline{\Omega}''}\int_{E''} G(\underline{r},E'',\underline{\Omega}'',t;\underline{R}')\Sigma_t(\underline{r},E'')C(E,\underline{\Omega};\underline{r},E'',\underline{\Omega}'')dE''d\underline{\Omega}''$$

$$= \delta(\underline{r}-\underline{r}')\delta(E-E')\delta(\underline{\Omega}-\underline{\Omega}')\delta(t-t') \quad , \quad (1)$$

where L is an operator as defined by Eq. (1). $\underline{R}$ is a shorthand notation denoting the neutron space position $\underline{r}$, its kinetic energy E, and direction of

*The shorthand notations "transport equation" and "adjoint equation" will be used rather than "neutron transport equation" and "adjoint neutron transport equation," respectively.

motion $\underline{\Omega}$ at time t. $C(E,\underline{\Omega};\underline{r},E'',\underline{\Omega}'')dEd\underline{\Omega}$ is the number of neutrons emerging in the phase-space volume dE about E and in $d\underline{\Omega}$ about $\underline{\Omega}$ following a collision of a neutron with energy E'' and direction of motion $\underline{\Omega}''$. Processes such as fission and elastic and inelastic scattering are included so that the collision kernel C usually will not be a normalized density function. The total cross section Σ_t is assumed independent of time and of the direction of motion of the neutron so that the notations $\Sigma_t(\underline{R})$ and $\Sigma_t(\underline{r},E)$ are used interchangeably. The coordinates to the left of the semicolon in the Green's function G of Eq. (1) represent field (i.e., final-state) points, and those to the right of the semicolon represent source points so that $G(\underline{R};\underline{R}')$ is the neutron flux at $\underline{R}$ due to a unit point source at $\underline{R}'$.

The neutron flux $\varphi(\underline{R})$ may be expressed in terms of the solution of Eq. (1) for the Green's function as

$$\varphi(\underline{R}) = \int G(\underline{R};\underline{R}')S(\underline{R}')d\underline{R}' \quad , \quad (2)$$

where $S(\underline{R}')$ is the extraneous source density. However, rather than using the Monte Carlo method to compute a point value of the neutron flux, we more often use it to estimate a functional J (or a number of such functionals) defined as

$$J = \int \varphi(\underline{R})\Sigma(\underline{R})d\underline{R}$$

$$= \iint G(\underline{R};\underline{R}')S(\underline{R}')\Sigma(\underline{R})d\underline{R}'d\underline{R} \quad . \quad (3)$$

Here, $\Sigma(\underline{R})$ is an arbitrary "cross section" of interest and the last relation of Eq. (3) was obtained by utilizing the expression for the neutron flux as given by Eq. (2). An estimate of the functional J with Monte Carlo may be obtained by selecting the i'th source neutron coordinates $\underline{R}_i$ with the density function $S(\underline{R}')$ and following the subsequent history of the neutron (and progeny) to compute the estimate

$$J_i = \int G(\underline{R};\underline{R}_i)\Sigma(\underline{R})d\underline{R}\ W(\underline{R}_i) \quad , \quad (4)$$

where $W(\underline{R}_i)$ is the initial weight assigned to the neutron as given by $\int S(\underline{R}')d\underline{R}'$. The estimate of J, as given by Eq. (4), is obtained by sampling from the transport equation, but a corresponding estimate

of J may be obtained by sampling from the adjoint equation.

The adjoint equation for the adjoint Green's function G^+ is obtained by finding an operator L^+ that satisfies the equation

$$\int \left[L^+ G^+(\underline{R};\underline{R}')\right] G(\underline{R};\underline{R}') d\underline{R} = \int G^+(\underline{R};\underline{R}')[LG(\underline{R};\underline{R}')] d\underline{R} \quad . \tag{5}$$

The boundary conditions on $G^+(\underline{R};\underline{R}')$ are chosen to be consistent with those on $G(\underline{R};\underline{R}')$ and are such that the bilinear concomitant[8] is zero. The definition of the operator L^+ in Eq. (5) with the associated boundary conditions is used to obtain the adjoint equation as

and then following the subsequent history of the pseudoneutron (and progeny) to compute the estimate

$$J_i = \int G^+(\underline{R}';\underline{R}_i) S(\underline{R}') d\underline{R}' \, W(\underline{R}_i) \quad , \tag{10}$$

where $W(\underline{R}_i)$ is the initial weight assigned to the pseudoneutron as given by $\int \Sigma(\underline{R}') d\underline{R}'$. The roles of the neutron source S and the scoring cross section Σ have been interchanged in this estimation of J by sampling from the adjoint equation. Σ now assumes the role of a "source" and S the role of a scoring "cross section." This fact has two well-known implications about the computational effort required for a problem. (1) If a response of some part of the system as a function of the neutron source dis-

$$L^+ G^+(\underline{R};\underline{R}') = -\frac{1}{v} \frac{\partial G^+(\underline{R};\underline{R}')}{\partial t} - \underline{\Omega} \cdot \underline{\nabla} G^+(\underline{R};\underline{R}') + \Sigma_t(\underline{R}) G^+(\underline{R};\underline{R}')$$

$$- \int_{\Omega''} \int_{E''} G^+(\underline{r},E'',\underline{\Omega}'',t;\underline{R}') \Sigma_t(\underline{r},E'') \left[\frac{C(E'',\underline{\Omega}'';\underline{r},E,\underline{\Omega}) \Sigma_t(\underline{r},E)}{\Sigma_t(\underline{r},E'')}\right] dE'' d\underline{\Omega}'' = \delta(\underline{r} - \underline{r}') \delta(E - E') \delta(\underline{\Omega} - \underline{\Omega}') \delta(t - t'). \tag{6}$$

A reciprocity relation between G^+ and G may be derived by multiplying Eq. (6) (with the source at an arbitrary point $\underline{R}'''$ rather than $\underline{R}'$) by $G(\underline{R};\underline{R}') d\underline{R}$, multiplying Eq. (1) by $G^+(\underline{R};\underline{R}''') d\underline{R}$, extracting the difference of the resulting two equations, and integrating this difference over all of phase space. Then the subsequent interchange of variables, replacing $\underline{R}'$ by $\underline{R}$ and $\underline{R}'''$ by $\underline{R}'$, yields the familiar form of the reciprocity theorem,

$$G^+(\underline{R}';\underline{R}) = G(\underline{R};\underline{R}') \quad . \tag{7}$$

The reciprocity relation of Eq. (7) may be inserted into Eq. (3) to obtain an alternative expression for the functional J as

$$J = \int\int G^+(\underline{R}';\underline{R}) S(\underline{R}') \Sigma(\underline{R}) d\underline{R}' d\underline{R} \quad . \tag{8}$$

The functional J of Eq. (8) may be estimated with Monte Carlo by selecting the i'th source pseudoneutron* coordinates $\underline{R}_i$ with the density function

$$\Sigma(\underline{R})/\int \Sigma(\underline{R}') d\underline{R}' \tag{9}$$

tribution is required, it may be more efficient to estimate the functionals by sampling from the adjoint equation. This is because only one adjoint calculation is required rather than a number of separate transport calculations. (2) If the phase-space volume containing nonzero Σ is small, it may be more efficient to estimate J by sampling from the adjoint equation because all pseudoneutron histories begin in the small phase-space volume.

These advantages obtained by sampling from the adjoint equation are expected to accrue when the phase-space volume, where the neutron source is nonzero, is not too small* and if a reasonably efficient scheme is available for sampling from the adjoint equation.

B. Sampling from the Adjoint Equation

The approach used here to develop a scheme for sampling from the adjoint equation is to begin by finding a simple transformation that will transform the adjoint equation, Eq. (6), into an equation identical in form to the transport equation, Eq. (1). Techniques for sampling from this transformed

---

*Pseudoneutrons are defined here as those "particles" whose transport is described by the adjoint equation.

*Point neutron sources may be treated with a special point source estimator discussed in Appendix E.

equation are well known from the wealth of experience obtained by sampling from the transport equation.

The simple transformation is obtained with the definitions

$$t_a = t_m - t$$

$$\underline{\Omega}_a = -\underline{\Omega}$$

$$G_a^+(\underline{r},E,\underline{\Omega}_a,t_a;\underline{r}',E',\underline{\Omega}_a',t_a')$$

$$= G^+(\underline{r},E,-\underline{\Omega}_a,t_m - t_a;\underline{r}',E',-\underline{\Omega}_a',t_m - t_a') \quad , \quad (11)$$

where t_m is a maximum time of interest in the problem, t_a will be the adjoint time, and $\underline{\Omega}_a$ will be the direction of motion of the pseudoneutron. Substitution of these definitions into Eq. (6) yields the transformed equation

$$\frac{1}{v}\frac{\partial G_a^+(R_a;\underline{R}_a')}{\partial t_a} + \underline{\Omega}_a \cdot \underline{\nabla}G_a^+(R_a;R_a') + \Sigma_t(\underline{R}_a)G_a^+(\underline{R}_a;R_a')$$

$$- \int_{\underline{\Omega}_a''}\int_{E''} G_a^+(\underline{r},E'',\underline{\Omega}_a'',t_a;\underline{R}_a')\Sigma_t(\underline{r},E'')\left[\frac{C(E'',-\underline{\Omega}_a'';\underline{r},E,-\underline{\Omega}_a)\Sigma_t(r,E)}{\Sigma_t(\underline{r},E'')}\right] dE''\ d\underline{\Omega}_a'' = \delta(\underline{r}-\underline{r}')\delta(E-E')\delta(-\underline{\Omega}_a+\underline{\Omega}_a')\delta(-t_a+t_a'),$$

$$(12)$$

where $\underline{R}_a$ is defined to be the phase-space point $r,E,\underline{\Omega}_a,t_a$. Equation (12) is identical in form to the neutron transport equation, where the term in brackets in the integrand represents the transfer kernel.

It may also be proved that G_a^+ satisfies the same boundary conditions as G. The boundary condition for G is that $G(\underline{r}_s,E,\underline{\Omega}^-,t;\underline{R}') = 0$ at every point $\underline{r}_s$ on the outer surface of the system, where $\underline{\Omega}^-$ denotes any direction into the system. This boundary condition on G combined with the requirement that the bilinear concomitant be zero on the outer surface leads to the boundary condition for G^+ of[8]

$$G^+(\underline{r}_s,E,\underline{\Omega}^+,t;\underline{R}') = 0 \quad , \quad (13)$$

where $\underline{\Omega}^+$ denotes any direction out of the system. Owing to the definition of G_a^+ in Eq. (11) and the boundary condition on G^+ in Eq. (13), the boundary condition on G_a^+ is that no pseudoneutrons enter the system from the outer surface. The time boundary

condition on G is that $G(\underline{R};\underline{R}') = 0$ for $t' > t$. This boundary condition coupled with the reciprocity theorem of Eq. (7) and the definitions in Eq. (11) requires that $G_a^+(\underline{R}_a;\underline{R}_a') = 0$ for $t_a' > t_a$.

Because Eq. (12) has the same form as the neutron transport equation and satisfies the same type of boundary conditions, a possible scheme for estimating the functional J of Eq. (8) is as follows.

1. Select the initial coordinates $\underline{R}_i$ of the pseudoneutron from the density function (see expression (9)),

$$g(\underline{R}_a) = \frac{\Sigma(\underline{r},E,-\underline{\Omega}_a,t_m - t_a)}{\int\Sigma(\underline{r}',E',-\underline{\Omega}_a',t_m - t_a')d\underline{R}_a'} \quad , \quad (14)$$

with the initial weight of the pseudoneutron given by W as

$$W = \int\Sigma(\underline{r}',E',-\underline{\Omega}_a',t_m - t_a')d\underline{R}_a' \quad . \quad (15)$$

2. Sample for the distance to collision χ with the exponential density function,

$$T(\chi) = \Sigma_t(\chi)e^{-\int_0^\chi \Sigma_t(\chi')d\chi'} \quad , \quad (16)$$

where this density function is determined along the direction of flight of the pseudoneutron and $\chi = 0$ is the previous collision point.

3. Each collision of the i'th pseudoneutron history (or its progeny) contributes to the estimate of the function J_i as

$$J_i = J_i' + W\ S(\underline{r},E,-\underline{\Omega}_a,t_m - t_a)/\Sigma_t(\underline{r},E) \quad , \quad (17)$$

where J_i' is the sum of the tabulations from previous collisions. Here a volumetric source S is assumed. The scoring is different for a surface source as is discussed in Sec. III.

4. At each collision of the pseudoneutron with a precollision energy E', direction of motion $\underline{\Omega}_a'$, and weight W', sample for the new energy E and

4

direction of motion $\underline{\Omega}_a$ with the density function

$$f(E,\underline{\Omega}_a;\underline{r},E',\underline{\Omega}'_a)$$

$$= \frac{C(E',-\underline{\Omega}'_a;\underline{r},E,-\underline{\Omega}_a)\Sigma_t(\underline{r},E)}{\int_{\underline{\Omega}''}\int_{E''}C(E',-\underline{\Omega}'_a;\underline{r},E'',-\underline{\Omega}''_a)\Sigma_t(\underline{r},E'')dE''\,d\underline{\Omega}''_a} \quad . \quad (18)$$

The new weight of the pseudoneutron is then obtained as

$$W = \frac{W'\int_{\underline{\Omega}''}\int_{E''}C(E',-\underline{\Omega}'_a;\underline{r},E'',-\underline{\Omega}''_a)\Sigma_t(\underline{r},E'')dE''\,d\underline{\Omega}''_a}{\Sigma_t(\underline{r},E')} \quad . \quad (19)$$

5. Return to step 2 if the pseudoneutron energy is less than the maximum energy of interest and if the time t_a is less than t_m. Otherwise, terminate the history with the estimate of the functional J for this history given by J_i.

We will call the scheme outlined above an analog scheme for sampling from the adjoint equation because it is similar to an analog scheme for sampling from the transport equation. The distance-to-collision density function $T(\chi)$ of Eq. (16) is identical to the corresponding density function utilized for sampling from the transport equation. The roles of the scoring cross section Σ and the source S are interchanged in Eqs. (14) and (17) from their corresponding roles when sampling from the transport equation. The most important difference between the two analog sampling schemes involves the density functions for selecting the energy and direction of motion after a collision, $f(E,\underline{\Omega}_a;\underline{r},E',\underline{\Omega}'_a)$ of Eq. (18) for sampling from the adjoint equation, and the normalized form of the collision kernel $C(E,\underline{\Omega};\underline{r},E',\underline{\Omega}')$ for sampling from the transport equation. Not only does the density function f of Eq. (18) have the additional multiplier Σ_t, but also the primed and unprimed variables of the energy and direction of motion in the arguments of C (the negative signs in the direction coordinates are not considered important in this treatment because we will consider isotropic media) are interchanged from their corresponding role when sampling from the transport equation.

If the analog scheme is to be utilized to sample from the adjoint equation, these differences between the density function $f(E,\underline{\Omega}_a;\underline{r},E',\underline{\Omega}'_a)$ and the normalized form of the collision kernel $C(E,\underline{\Omega};\underline{r},E',\underline{\Omega}')$ dictate the need for data that are not available in a cross-section library that is constructed for sam-

pling from the transport equation. To see what additional data are needed and to eventually introduce the sampling scheme used in the MCNA code, we will now consider the practical aspects of sampling with the density function f.

It is convenient to express the collision kernel C as a sum of the respective contributions of possible events α as

$$C(E',-\underline{\Omega}'_a;\underline{r},E,-\underline{\Omega}_a) = \sum_\alpha \frac{\Sigma_\alpha(\underline{r},E)}{\Sigma_t(\underline{r},E)}\,C_\alpha(E',-\underline{\Omega}'_a;\underline{r},E,-\underline{\Omega}_a)\;,$$
$$(20)$$

where Σ_α is the macroscopic cross section for an event α and C_α is the corresponding collision kernel for the event α. The events α may be chosen to correspond to the physical processes; for example, elastic scattering with a given isotope. Alternatively, the events may be defined less conventionally, for example, the event defined as an inelastic scattering with any of the isotopes present, subject to the restriction that the (pseudo) neutron is scattered to an energy between two given limits.

The expansion of C, as given by Eq. (20), may be substituted into the density function f of Eq. (18) to obtain

$$f(E,\underline{\Omega}_a;\underline{r},E'\cdot\underline{\Omega}'_a) = \sum_\alpha Q_\alpha(\underline{r},E',\underline{\Omega}'_a)f_\alpha(E,\underline{\Omega}_a;\underline{r},E',\underline{\Omega}'_a)\;,$$
$$(21)$$

where Q_α and f_α are defined as

$$Q_\alpha(\underline{r},E',\underline{\Omega}'_a)$$

$$= \frac{\int_{\underline{\Omega}_a}\int_E C_\alpha(E',-\underline{\Omega}'_a;\underline{r},E,-\underline{\Omega}_a)\Sigma_\alpha(\underline{r},E)dEd\underline{\Omega}_a}{\sum_{\alpha'}\int_{\underline{\Omega}''_a}\int_{E''}C_{\alpha'}(E',-\underline{\Omega}'_a;\underline{r},E'',-\underline{\Omega}''_a)\Sigma_{\alpha'}(\underline{r},E'')dE''\,d\underline{\Omega}''_a}$$
$$(22)$$

and

$$f_\alpha(E,\underline{\Omega}_a;\underline{r},E'\cdot\underline{\Omega}'_a)$$

$$= \frac{C_\alpha(E',-\Omega';\underline{r},E,-\underline{\Omega}_a)\Sigma_\alpha(\underline{r},E)}{\int_{\underline{\Omega}''_a}\int_{E''}C_\alpha(E',-\underline{\Omega}'_a;\underline{r},E'',-\underline{\Omega}''_a)\Sigma_\alpha(\underline{r},E'')dE''d\underline{\Omega}''_a}\quad .$$
$$(23)$$

The energy E and direction of motion $\underline{\Omega}_a$ may be sampled with the density function f of Eq. (21) by

selecting event α with probability Q_α and subsequently selecting the energy E and direction of motion $\underline{\Omega}_a$ from the density function f_α. Thus, the data required in a cross-section library would be the probabilities of events as given by the Q_α of Eq. (22) and the corresponding conditional density functions as given by the f_α of Eq. (23).

Two difficulties are evident in this analog scheme for sampling from the adjoint equation. (1) A considerable amount of effort would be required to create a new library containing the f_α and Q_α functions in an acceptable format for sampling, and (2) the analog scheme for sampling from the adjoint equation may be inefficient owing to statistical errors due to an unacceptably large theoretical variance of the individual samples. One can reduce this variance by properly altering the sampling scheme and adjusting the pseudoneutron weight to obtain an unbiased estimate. The unbiased estimate is obtained by multiplication of the analog pseudoneutron weight by the ratio of the analog density function to the alternate density function at each sampling. For example, if some functions $\overline{f}_\alpha$ and $\overline{Q}_\alpha$ are used for sampling rather than the analog density functions f_α and Q_α, the pseudoneutron weight is obtained from the analog weight of Eq. (19) and the ratio of the density functions as

functional. There is usually a trade-off between the theoretical variance per individual random sample and the computation time required to sample from the density functions. The MCNA code utilizes a coupled sampling approach to try to compromise on these requirements.

C. Coupled Sampling

It is well known that a theoretical "zero-variance" scheme exists for estimating the functional J by sampling from the adjoint equation. The zero-variance scheme depends upon the neutron flux and thus is impractical to utilize exactly, but this does suggest the possibility of a coupled sampling approach to obtain an approximation to the zero-variance scheme.

The coupled sampling as developed here consists of sampling from the transport equation to construct an approximation to the theoretical zero-variance scheme and then using this approximate scheme to estimate the functional J by sampling from the adjoint equation. We will now give expressions for the zero-variance density functions and briefly discuss how sampling from the transport equation may be used to obtain approximations to them. The actual techniques used in the MCNA code are given in Sec. III.

The functions g_0, Q_{∞} and f_{∞} are defined to

$$\overline{W} = \overline{W}' \frac{\int_{\underline{\Omega}_a''} \int_{E''} C(E', -\underline{\Omega}_a'; \underline{r}, E'', -\underline{\Omega}_a'') \Sigma_t(\underline{r}, E'') dE'' d\underline{\Omega}_a''}{\Sigma_t(\underline{r}, E)} \left\{ \frac{f_\alpha(E, \underline{\Omega}_a; \underline{r}, E', \underline{\Omega}')}{\overline{f}_\alpha(E, \underline{\Omega}_a; \underline{r}, E', \underline{\Omega}_a')} \frac{Q_\alpha(\underline{r}, E', \underline{\Omega}_a)}{\overline{Q}_\alpha(\underline{r}, E', \underline{\Omega}_a')} \right\}$$

$$= \overline{W}' \frac{C_\alpha(E', -\underline{\Omega}_a'; \underline{r}, E, -\underline{\Omega}_a) \Sigma_\alpha(\underline{r}, E)}{\Sigma_t(\underline{r}, E') \overline{Q}_\alpha(\underline{r}, E', \underline{\Omega}_a') \overline{f}_\alpha(E, \underline{\Omega}_a; \underline{r}, E', \underline{\Omega}_a')} \quad , \qquad (24)$$

where α, E, and $\underline{\Omega}_a$ were selected in the sampling.

A density function for the alternate sampling scheme may be chosen arbitrarily from the set of density functions that are nonzero at each point where the corresponding analog density function is nonzero. Use of the correct weight multiplier ensures an unbiased estimate for any such density functions. However, the variance in the estimate of the functional J depends upon the density functions chosen for the sampling scheme, so the density functions should be chosen to minimize the computation effort for a given precision in the estimate of the

be the density functions of the zero-variance scheme which are utilized to sample for the same random variables as the density functions g, f_α, and Q_α, respectively, of the analog scheme. The derivation of this zero-variance scheme will not be given here because it is available in the literature.[9,10] The zero-variance density functions of interest here are

$$g_0(R_a) = \frac{\Sigma(\underline{r}, E, -\underline{\Omega}_a) \varphi(\underline{r}, E, -\underline{\Omega}_a)}{\iiint \Sigma(r', E', -\underline{\Omega}_a') \varphi(\underline{r}, E', -\underline{\Omega}_a') d^3r' dE' d\underline{\Omega}_a'} \quad ,$$

$$(25)$$

$$Q_{\alpha0}(\underline{r},E',\underline{\Omega}_a') = \frac{\int_{\underline{\Omega}_a}\int_E C_\alpha(E',-\underline{\Omega}_a';\underline{r},E,-\underline{\Omega}_a)\Sigma_\alpha(\underline{r},E)\varphi(\underline{r},E,-\underline{\Omega}_a)dEd\underline{\Omega}_a}{\sum_{\alpha'}\int_{\underline{\Omega}_a''}\int_{E''} C_{\alpha'}(E',-\underline{\Omega}_a';\underline{r},E'',-\underline{\Omega}_a'')\Sigma_{\alpha'}(\underline{r},E'')\varphi(\underline{r},E'',-\underline{\Omega}_a'')dE''d\underline{\Omega}_a''} \quad , \tag{26}$$

$$f_{\alpha0}(E,\underline{\Omega}_a;\underline{r},E',\underline{\Omega}_a') = \frac{C_\alpha(E',-\underline{\Omega}_a';\underline{r},E,-\underline{\Omega}_a)\Sigma_\alpha(\underline{r},E)\varphi(\underline{r},E,-\underline{\Omega}_a)}{\int_{\underline{\Omega}_a}\int_{E''} C_\alpha(E',-\underline{\Omega}_a';\underline{r},E'',-\underline{\Omega}_a')\Sigma_\alpha(\underline{r},E'')\varphi(\underline{r},E'',-\underline{\Omega}_a'')dE''d\underline{\Omega}_a} \quad , \tag{27}$$

where the density functions have been assumed to depend only weakly on time so the time variable has been suppressed. The density function of the zero-variance scheme for selecting the distance to collision is not given here because we assume that the use of the analog exponential density function of Eq. (16) with the added option of splitting or "Russian roulette" is sufficient for most purposes.

The density functions of Eqs. (25) to (27) have an interesting physical significance. The optimal sampling requires that, in the adjoint solution, regions of phase space be sampled proportional to the rate at which the reverse (neutron) processes are occurring. This provides a helpful picture for obtaining useful approximations to the zero-variance density functions when sampling from the transport equation. Such a physical aid is useful because it is clear that, in addition to the problem of statistical fluctuations in the evaluation of $f_{\alpha0}$ and $Q_{\alpha0}$ by sampling from the transport equation, some phase-space averaging must be incorporated to reduce the computer memory requirements for tabulating these functions. The averaging techniques used in MCNA are formulated to optimize the selection of the pseudoneutron energy. These averaging techniques and a general discussion of the MCNA code are given in the next section.

III. DESCRIPTION OF MCNA

The computer code MCNA for solving the adjoint equation with the Monte Carlo method was constructed by modifying the computer code MCN;[4-6] MCN solves the transport equation with Monte Carlo. The geometry routines and cross-section models are identical in the two codes. The cross-section libraries have the same format. However, the actual cross sections for reactions are always tabulated in the MCNA library, while probabilities of reactions are sometimes tabulated in the MCN cross-section library.

Figure 1 illustrates the steps in the solution of a problem with the MCNA code. The initiation of the problem in Step 1 is identical to the initiation in the MCN code.[4-6] The sampling from the transport equation in Step 3 is also identical to the MCN program with two exceptions: (1) the program has been altered to allow cross-section data rather than probabilities of reactions to be used in the sampling, and (2) density functions are computed for a subsequent sampling from the adjoint equation. The rest of the discussion in this section will concentrate on this latter difference and on steps 2, 4, and 5 of Fig. 1.

The zero-variance functions, $Q_{\alpha0}$ of Eq. (26) and $f_{\alpha0}$ of Eq. (27), are approximated in the sampling from the transport equation by first separating three-dimensional Euclidean space and the energy coordinate into contiguous segments. The Euclidean space segments are assumed to correspond to the physical cells (regions) of the system. An energy, directional, and spatial averaging of the $Q_{\alpha0}$ in Eq. (26) is performed over each phase-space segment in the Monte Carlo sampling from the transport equation. These average quantities are denoted by $\overline{Q}_\alpha(j,k,\cdots)$, where j is an integer denoting the energy segment, k is an integer denoting the cell, and the $\cdots$ indicates that (depending upon the type of event) other integers may also be used. Thus, the $\overline{Q}_\alpha(j,k,\cdots)$ represents a Monte Carlo phase-space average of $Q_{\alpha0}(\underline{r},E',\underline{\Omega}_a')$.

Four general types of events, designated by α, are utilized in MCNA. Note that these events were selected for convenience in the sampling and often represent a sum of some possible reactions. The four events with their corresponding physical interpretations in the sampling from the transport equation are as follows.
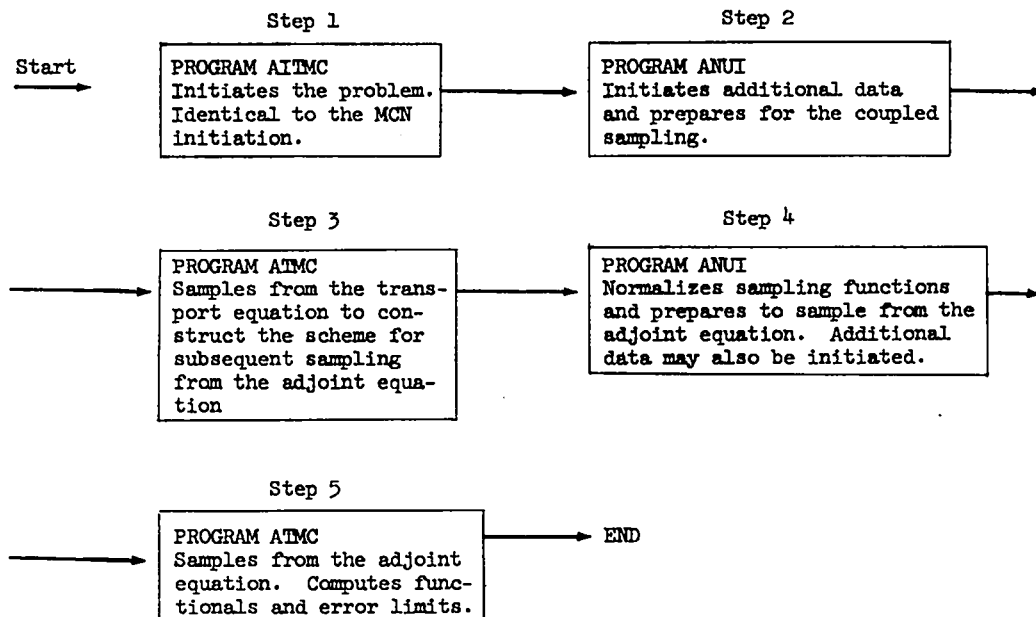
Fig. 1. Brief flow diagram of a computation with the MCNA code.

1. Elastic scattering with an isotope i. This type of event is designated by $\alpha = 1$, and $\overline{Q}_1(j,k,i)$ is proportional to the number of neutrons that suffer an elastic collision in cell k with isotope i and are scattered into energy group j.

2. Inelastic scattering with a continuum density function (i.e., not a discrete level in the laboratory or center-of-mass system) to describe the energy transfer. This type of event is designated by $\alpha = 2$, and $\overline{Q}_2(j,k,\beta)$ is proportional to the number of neutrons that scatter into energy group j, given that the originating neutrons suffered inelastic collisions (fission not included) in cell k with a continuum density function utilized to describe the energy transfer, where the neutron loss of energy in the laboratory system is within an energy band designated by the integer β.

3. Inelastic scattering with a discrete model (in the laboratory or center-of-mass system) to describe the energy transfer. This type of event is designated by $\alpha = 3$, and $\overline{Q}_3(j,k,i,\ell)$ is proportional to the number of neutrons that scatter into energy group j, given that the originating neutrons suffered an inelastic scattering collision in cell k with discrete level ℓ of isotope i.

4. Fission. This type of event is designated by $\alpha = 4$, and $\overline{Q}_4(j,k,\gamma)$ is proportional to the num-

ber of neutrons born from fission into energy group j and cell k, where the parent neutrons were in energy group γ when fission occurred.

The indices in these definitions assume all integer values that are within the bounds:

$1 \leq i \leq$ (number of isotopes in cell k),

$1 \leq j \leq J$, where J is the number of energy groups used in the subsequent sampling from the adjoint equation,

$1 \leq k \leq$ (number of cells),

$1 \leq \beta \leq$ (number of energy bands for energy group j),

$1 \leq \ell \leq$ (number of discrete levels for isotope i and energy group j),

$1 \leq \gamma \leq J$.

These physical definitions of the $\overline{Q}_\alpha$'s are used to evaluate them by sampling from the transport equation. The word "proportional" is used because the $\overline{Q}_\alpha$'s must be normalized before the subsequent sampling from the adjoint equation. Hence, for a given j and k, the $\overline{Q}_\alpha$'s are normalized with the condition

$$\sum_i \overline{Q}_1(j,k,i) + \sum_\beta \overline{Q}_2(j,k,\beta) + \sum_{i,\ell} \overline{Q}_3(j,k,i,\ell)$$

$$+ \sum_\gamma \overline{Q}_4(j,k,\gamma) = 1 \quad . \qquad (28)$$

In the subsequent sampling from the adjoint equation, J is the energy group of the pseudoneutron before a collision and each $Q_\alpha(j,k,\cdots)$ is the probability that it will suffer that event. Although a form of multigroup treatment is used to determine the type of event that occurs, this is not a multigroup treatment in the usual sense because the final pseudoneutron energy after the event is selected from a continuous distribution (except, of course, for a discrete inelastic scattering in the laboratory system).

The conditional $\bar{f}_\alpha$ density functions for sampling the energy and direction of flight of the pseudoneutron, given that the event α occurs, (in some cases these $\bar{f}_\alpha$'s are also computed by sampling from the transport equation) are discussed in Appendix A. The weights of the pseudoneutron after each event α are also derived in Appendix A.

The format of the input data in the MCNA code is identical to that of the input data in the MCN code. The input data are discussed in Appendix B.

Most of the effort required to set up a problem with the MCNA code is usually involved with the construction of the sources for sampling from the transport and adjoint equations and the scoring routine for tabulating the functional(s). The neutron source routine for the sampling from the transport equation is constructed as in the MCN code; i.e., simple routines are available in the code, or more complicated routines may be written by the user. However, for problems in which a number of functionals are being computed in the sampling from the adjoint equation, some care should be taken in choosing the source for the transport portion of the calculation. Generally, the density function for selecting the energy of the source neutron should emphasize the upper portion of the energy spectra of the functionals.

A pseudoneutron source routine is also available in the MCNA code for simple sources, but a separate routine, ASOURC, must be written for complicated sources. To illustrate the procedure for setting up the adjoint source, we begin with the density function $g(\underline{R}_a)$ of Eq. (14). The MCNA code uses real time t in the adjoint calculation rather than the adjoint time t_a, so g is expressed as

$$g(\underline{r},E,\underline{\Omega}_a,t) = \frac{\sum(\underline{r},E,-\underline{\Omega}_a,t)}{\iiiint \sum(\underline{r}',E',-\underline{\Omega}_a',t')d^3r'dE'd\underline{\Omega}_a'dt'} .$$

(29)

The corresponding zero-variance density function g_0 of Eq. (25) depends upon the neutron flux $\varphi(\underline{r},E,-\underline{\Omega}_a,t)$. When information on the general behavior of the neutron flux is available, it should be used to construct a near-optimal density function. For illustration, we will assume that such information is not available and that our primary interest is to find a simple method to select the initial pseudoneutron coordinates. The following method is quite general, although it is not optimal from a minimum-variance viewpoint.

The density function g may be difficult to sample owing to the behavior of the cross section Σ. An alternative is to sample from a density function $\bar{g}$ that is easy to sample from and is zero only in regions of phase space where Σ is zero. An unbiased estimate is obtained by assigning the pseudoneutron an initial weight of

$$\bar{W} = \frac{\Sigma(\underline{r},E,-\underline{\Omega}_a,t)}{\bar{g}(\underline{r},E,\underline{\Omega}_a,t)} ,$$

(30)

where r, E, $\underline{\Omega}_a$ and t were selected with the density function $\bar{g}$.

For example, assume that

$$\Sigma(\underline{r},E,-\underline{\Omega}_a,t) = \Sigma(E) \quad \text{for } \underline{r} \text{ in a volume}$$
$$V, E_1 < E < E_2, \text{ and}$$
$$t_1 < t < t_2,$$
$$= 0 \text{ otherwise,}$$

and that we choose the density function $\bar{g}$ as

$$\bar{g}(\underline{r},E,\underline{\Omega}_a,t) = \frac{1}{4\pi} \frac{1}{(E_2 - E_1)} \frac{1}{V} \frac{1}{(t_2 - t_1)} ,$$

(31)

$$\text{for } \underline{r} \text{ in a volume } V, E_1 < E < E_2,$$
$$\text{and } t_1 < t < t_2,$$
$$= 0 \text{ otherwise.}$$

The pseudoneutron source routine would

1. select the initial position z, y, z from a uniform distribution in the volume V,

2. select the direction cosines u, v, w from an isotropic distribution in the laboratory system,

3. select the energy E from a uniform distribution between E_1 and E_2,

4. select the time t from a uniform distribution between t_1 and t_2, and

5. assign the pseudoneutron an initial weight, obtained from Eq. (30), of

$$\overline{W} = \Sigma(E)4\pi(E_2 - E_1)V(t_2 - t_1) \quad . \quad (32)$$

A subroutine called SCORE(KASR) must be supplied by the user to tabulate the contribution of each pseudoneutron history to the functional(s). The parameter KASR is used to convey what is happening to the pseudoneutron each time the subroutine is called by the main program. Subroutine SCORE is called with KASR = 1 each time a pseudoneutron suffers a collision. The variables X, Y, Z, U, V, W, ERG, VL, IA, JA, TME, PL, and WT are the parameters describing the pseudoneutron at the collision. Here, X, Y, Z are the spatial Euclidean coordinates, u, v, w are the direction-of-motion cosines, ERG is the kinetic energy, VL is the velocity, IA is the program cell number, JA is the program surface number (if needed), TME is the time, PL is the macroscopic cross section, and WT is the weight of the pseudoneutron. Subroutine SCORE is called with KASR = 2 each time a pseudoneutron crosses a surface boundary. The previously named variables are the parameters of the pseudoneutron at the surface crossing. Subroutine SCORE is called with KASR = 3 for the point-source estimator discussed in Appendix E. A special "last-flight" scoring surface option, denoted by the first data entry of card ALE* greater than zero, is also available in MCNA. If this is used, subroutine SCORE is called each time the pseudoneutron energy is within a designated energy bin and the projected line of flight crosses a designated surface. The previously named variables are the parameters at the crossing of the designated surface, and KASR is equal to 4.

The actual scoring proceeds as in a Monte Carlo transport calculation except that the source S assumes the role of a scoring cross section. The i'th pseudoneutron history is used to estimate J_i of Eq. (10), which may be expressed as

The definitions in Eq. (11) have been used to express J_i in this form.

The source is usually distributed either in a volume of Euclidean space or on a surface. We now consider these two types of sources.

The transformed adjoint Green's function G_a^+ satisfies an equation of the same form as the neutron transport equation. Thus, the number of collisions occuring in the phase-space volume d^3r about $\underline{r}$, dE about E, $d\underline{\Omega}_a$ about $\underline{\Omega}_a$, and dt_a about t_a is given by

$$G_a^+(\underline{r},E,\underline{\Omega}_a,t_a;\underline{r}_i,E_i,\underline{\Omega}_{ai},t_{ai})\Sigma_t(\underline{r},E)d^3rdEd\underline{\Omega}_adt_a \quad . \quad (34)$$

The contribution of this volume of phase space (in the limit as the phase-space volume approaches zero) to J_i is given by

$$\begin{pmatrix} \text{Number of collisions} \\ \text{occurring in the small} \\ \text{phase-space volume due} \\ \text{to a unit source at } \underline{R}_i \end{pmatrix} \quad S(\underline{r},E,-\underline{\Omega}_a,t)/\Sigma_t(r,E) \quad . \quad (35)$$

The number of collisions occuring in the small phase-space volume due to a source at $\underline{R}_i$ of strength $W(R_i)$ is just the sum of the weights of the pseudoneutron each time it suffers a collision in the small phase-space volume. Thus, the contribution of each pseudoneutron collision to the functional is

$$\overline{W}*S(\underline{r},E,-\underline{\Omega}_a,t)/\Sigma_t(\underline{r},E) \quad , \quad (36)$$

where $\overline{W}$ is the pseudoneutron weight at the collision point $r,E,\underline{\Omega}_a,t$. Here, $\underline{\Omega}_a$ is the direction of motion of the pseudoneutron before collision, so when S is not isotropic, the $\underline{\Omega}_a$ direction is reflected to determine S. The real time t, rather than the adjoint time t_a, is used in Eqs. (35) and (36) because the real time t is the time variable used in MCNA.

Subroutine SCORE is shown in Fig. 2 for a fictitious problem in which two unnormalized source spectra are of interest. These sources are denoted by S_1 and S_2 and are defined as

$$J_i = \int G_a^+(\underline{r},E,\underline{\Omega}_a,t_a;\underline{r}_i,E_i,\underline{\Omega}_{ai},t_{ai})S(\underline{r},E,-\underline{\Omega}_a,t_m - t_a)d^3rdEd\underline{\Omega}_adt_aW(\underline{R}_i) \quad . \quad (33)$$

*See Appendix B.

```
      SUBROUTINE SCORE(KASR)
C
C     INTEGER, DIMENSION, COMMON, AND EQUIVALENCE STATEMENTS ARE NOT
C     SHOWN, BUT CORRESPOND TO THOSE OF THE MAIN PROGRAM ATMC
C
C     SCORING FOR FICTITIOUS PROBLEM WITH VOLUME SOURCE
C     KASR = 1 DENOTES A COLLISION
C     IA = PROGRAM CELL NUMBER WHERE COLLISION OCCURS
C     TME = TIME AT COLLISION
C     ERG = PSEUDO-NEUTRON ENERGY AT COLLISION
C     WT = PSEUDO-NEUTRON WEIGHT AT COLLISION
C     4 PI = 12.5664
C     PL = MACROSCOPIC TOTAL CROSS SECTION IN CELL 9 FOR ENERGY ERG
C
      IF(KASR.NE.1) GO TO 25
      IF(IA.NE.9) GO TO 25
      IF(TME.LT.C.) GO TO 25
      IF(ERG.LT.1.) GO TO 25
      K = 1
      IF(ERG.LT.3.) GO TO 15
      K = 2
      IF(ERG.GT.6.) GO TO 25
   15 CONTINUE
      TSCOR(K) = TSCOR(K)+WT/(12.5664*ERG*PL)
   25 RETURN
      END
```

Fig. 2. Subroutine SCORE for a fictitious problem with a
source uniformly distributed in cell number 9.

$$S_1(\underline{r},E,\underline{\Omega},t) = \frac{1}{4\pi}\frac{1}{E} \quad \text{for} \quad \begin{cases} 0 < t < t_i, \\ 1. < E < 3., \text{ and} \\ \underline{r} \text{ in cell IA} = 9 \end{cases},$$

$$= 0 \quad \text{otherwise} \qquad (37)$$

$$S_2(\underline{r},E,\Omega,t) = \frac{1}{4\pi}\frac{1}{E} \quad \text{for} \quad \begin{cases} 0 < t < t_i, \\ 3. < E < 6., \\ \underline{r} \text{ in cell IA} = 9 \end{cases},$$

$$= 0 \quad \text{otherwise.}$$

Here, all pseudoneutrons are assumed to begin their life histories at the time t_i. Consequently, the maximum time is not checked in subroutine SCORE because the time t runs backward in the adjoint calculation.

When the neutron source S is on a surface, the space coordinate normal to the surface in Eq. (33) may be integrated readily because a delta function in the source is involved. The expression for J_i becomes

the source density per unit of area on the surface. Because the transformed adjoint Green's function G_a^+ satisfies an equation whose form is identical to the neutron transport equation, the number of "particles" crossing a phase-space element d^2r_s on the surface about $\underline{r}_s$ with energies in dE about E, direction of motion in $d\underline{\Omega}_a$ about $\underline{\Omega}_a$, and during a time dt_a about t_a is given by

$$\mu_n G_a^+(\underline{r}_s,E,\underline{\Omega}_a,t_a;\underline{r}_i,E_i,\underline{\Omega}_{ai},t_{ai})d^2r_s dEd\underline{\Omega}_a dt_a \quad , \quad (39)$$

where μ_n is the absolute value of the cosine of the angle between $\underline{\Omega}_a$ and a vector that passes through d^2r_s normal to the surface. Here we assume an infinitesimally small volume in phase space. Thus, the contribution of a pseudoneutron to the functional J_i each time it crosses the surface is given by

$$\overline{W}*S_s(\underline{r}_s,E,-\underline{\Omega}_a,t)/\mu_n \qquad (39a)$$

Subroutine SCORE is shown in Fig. 3 for a fictitious problem with a surface source S_s. We define the surface of the source to be a spherical surface of 12-cm radius and centered at x = 0, y = 0, and

$$J_i = \int G_a^+(\underline{r}_s,E,\underline{\Omega}_a,t_a;\underline{r}_i,E_i,\underline{\Omega}_{ai},t_{ai})S_s(\underline{r}_s,E,-\underline{\Omega}_a,t_m - t_a)d^2r_s dEd\underline{\Omega}_a dt_a \quad , \qquad (38)$$

where $\underline{r}_s$ denotes a point on the surface, d^2r_s denotes an element of area on the surface, and S_s is

```
      SUBROUTINE SCORE(KASR)
C
C     INTEGER, DIMENSION, CCMMCN, AND EQUIVALENCE STATEMENTS ARE NOT
C     SHOWN, BUT CORRESPEND TO THOSE OF THE MAIN PROGRAM ATMC
C
C     SCORING FOR FICTITIOUS PROBLEM WITH SURFACE SOURCE
C     KASR = 2 DENCTES A SURFACE CROSSING
C     JA = PROBLEM SURFACE NUMBER CROSSED
C     TMF = TIME AT SURFACE CRCSSING
C     ERG = PSEUDC-NEUTRCN ENERGY AT SURFACE CROSSING
C     WT = PSEUDC-NEUTRON WEIGHT AT SURFACE CROSSING
C     2 PI = 6.2832
C     X,Y,Z, ARE EUCLIDEAN COORDINATES OF THE PSEUDO-NEUTRON AT SURFACE
C     CROSSING
C     U,V,W ARE THE DIRECTION CF FLIGHT COSINES OF THE PSEUDO-NEUTRON
C     AT SURFACE CROSSING
C
      IF(KASR.NE.2) GO TO 25
      IF(JA.NE.6) GO TO 25
      IF(TMC.LT.C.) GO TO 25
      IF(ERG.LT.2.) GO TO 25
      IF(ERG.GT.4.) GO TO 25
      UNQR = (U*X+V*Y+W*Z)/12.
      IF(UNQR.LT.C.) GO TO 15
       TSCOR(1) = TSCOR(1) + WT*UNCR/(6.282*ERG)
      GO TO 25
   15 CONTINUE
      TSCOR(2) = TSCOR(2) + WT/(6.2832*ERG)
   25 RETURN
      END
```

Fig. 3. Subroutine SCORE for a fictitious problem with a
source uniformly distributed on surface number 6.

z = 0. The source density for this fictitious problem is defined as

$$S_s(\underline{r}_s,E,\underline{\Omega},t)=\frac{1}{2\pi}(\underline{\Omega}\cdot\underline{n})\frac{1}{E}\begin{cases}0<t<t_i,\\2.<E<4.,\\\underline{r}_s \text{ on surface } JA=6, \text{and}\\\underline{\Omega}\cdot\underline{n}>0\end{cases},$$

$$=\frac{1}{2\pi}(\underline{\Omega}\cdot\underline{n})^2\frac{1}{E}\begin{cases}0<t<t_i,\\2.<E<4.,\\\underline{r}_s \text{ on surface } JA=6, \text{and}\\\underline{\Omega}\cdot\underline{n}<0\end{cases},$$

$$= 0 \text{ otherwise.} \tag{40}$$

Here, $\underline{\Omega}$ is defined to be a unit vector, $\underline{n}$ is a unit vector normal to the surface in an outward direction, and all pseudoneutrons begin their life histories at t_i. For a pseudoneutron crossing the surface at x,y,z and with direction-of-motion coordinates, u, v,w, $\underline{\Omega}\cdot\underline{n}$ is given by

$$\underline{\Omega}\cdot\underline{n}=(\underline{i}u+\underline{j}v+\underline{k}v)\cdot(\underline{i}x+\underline{j}y+\underline{k}z)\Big/\sqrt{x^2+y^2+z^2}$$

$$= (ux+vy+wz)/12.. \tag{41}$$

If the neutron source S_s is isotropic, an infinite variance may occur in the estimate of the functional because the scoring is then inversly proportional to $|\underline{\Omega}\cdot\underline{n}|$. To avoid possible infinite variance, it is suggested that for $|\underline{\Omega}\cdot\underline{n}|$ values less than some small number ϵ (a value for ϵ is problem dependent, but $\epsilon=0.1$ should be satisfactory in most applications) the scoring should be inversely proportional to $\epsilon/2$.

This concludes the discussion of the MCNA program except for some additional considerations in the appendixes. A special distance-to-collision sampling option is discussed in Appendix C, and some miscellaneous probability concepts used in MCNA are discussed in Appendix D. Scoring in the adjoint calculation with a point neutron source is discussed in Appendix E. In Appendix F, the treatment of a neutron source containing a delta function in time is considered.

This discussion of MCNA has assumed a coupled sampling solution. There are problems of interest where some information about the energy dependence of the neutron flux is available. An option exists in MCNA to utilize this information to numerically construct the $\bar{Q}_\alpha$'s and thus, omit the sampling from

the transport equation. The numeric integration is then done in Step 2 of Fig. 1 and Steps 3 and 4 are bypassed.

The execution of an example problem with the coupled sampling method is discussed in the next section.

IV. EXAMPLE PROBLEM

We will comment on some tests of the programming reliability of the MCNA code before discussing the example problem.

It was impossible to completely check all aspects of MCNA for errors, and so a number of integral checks have been utilized. The integral checks were made between the MCNA and MCN programs. We assume here that MCN is a reliable program and so the

agreement of a number of computations with MCN and MCNA indicates the reliability of the MCNA program. Comparison of the results of two Monte Carlo programs has the disadvantage that statistical errors are involved in both answers; in the test calculations, the relative errors (standard deviation divided by the functional) are a few percent and in some cases less than 1%. We felt that the disadvantage of having statistical errors in the comparison code was more than offset by the advantage of using the same cross-section sets and interaction models.

Some of the comparisons made between the two computer program are summarized in Table I. A number of additional comparisons made on classified[13] problems have revealed a few minor errors in MCNA, which have been corrected.

TABLE I

SUMMARY OF INTEGRAL CHECKS ON THE MCNA PROGRAM

Geometrical Description	Functionals Computed	Comments
Point source of 12.2- to 15-MeV neutrons in infinite air; a shielding benchmark problem[(Ref.11)].	Neutron fluence as a function of energy and distance from the point source.	Agreement was obtained within statistical errors* for neutron energies of from 0.11 to 15.0 MeV and distances from the point source out to 1275 m. Standard deviations for high neutron energies ranged from ~ 1% near the source to 10% far from the source.
Near-critical sphere of 10% enriched uranium metal[(Ref.12)]. Delta function source at t = 0, of fission neutrons.	Total number of neutron collisions in the time interval from 80 to 96 shakes (~10 to 12 neutron generations) that occur in the energy interval from 0.5 to 1.5 MeV.	The result of the adjoint computation was 11.1 with a relative error of 9.6%, and the transport calculation yielded 12.8 with a relative error of 8.5%[(Ref.12)]. This is a better integral check than the relative errors indicate, owing to the large number of collisions between source particle and scoring. Any small errors in the adjoint sampling or computation of weight factors would be amplified.
Epithermal neutron source in an infinite medium of hydrogen at a temperature of 1.0 eV.	Neutron flux spectrum after the pulse has thermalized; also the total integral of the flux after thermalization.	The adjoint calculation was performed at 0.05-, 1.0-, 3.0-, and 10.0-eV energy points and agreed* with a Maxwellian flux to within relative errors of about 2.9%. The total integrals of the flux as computed with adjoint and transport Monte Carlo also agreed.* Here the relative errors in the adjoint and transport calculations were 1.4 and 0.52%, respectively.
Epithermal neutron source in an infinite medium of deuterium at a temperature of 1.0 eV.	Neutron flux spectrum after the pulse has thermalized; also the total integral of the flux after thermalization	Agreement with a Maxwellian flux to within relative errors of about 3%.

*Comparisons were made for 95% confidence limits.

The example problem is one of a set prompted by the need of the nuclear safeguards group to develop computational simulation of some experiments. These experiments involve a small amount of ^{235}U metal surrounded by a moderator. The delayed neutron response is measured after a pulse of neutrons is injected into the system.

This is a difficult problem to solve by a direct Monte Carlo calculation because the extraneous source is outside the system and only a small fraction of the source neutrons reach the small region of ^{235}U and cause fission. However, the computation of the number of first-generation fission neutrons produced in the small ^{235}U region is an excellent application of the adjoint approach because the histories of the pseudoneutrons begin in the small region of ^{235}U. It is straightforward to subsequently compute the number of delayed neutrons reaching a detector with a direct Monte Carlo calculation by using this first-generation fission source of neutrons.

The example problem is described in Table II.

TABLE II

DESCRIPTION OF THE EXAMPLE PROBLEM

Cell Descriptions (concentric spheres):

Cell Number	Inner Radius (cm)	Outer Radius (cm)	Element	Density (Atoms/barn-cm)
1	0.0	0.635	^{235}U	0.0478
2	0.635	8.255	H	0.0790
			C	0.0395
3	8.255	30.5	Void	----

Extraneous Neutron Sources:

$$S(\underline{r}_s, E, \underline{\Omega}) = \frac{1}{4\pi} \frac{1}{(3 \text{ MeV})} \frac{1}{4\pi |\underline{r}_s|^2} \text{ for } 12 \text{ MeV} < E < 15 \text{ MeV},$$

$$= 0 \text{ otherwise,}$$

where $\underline{r}_s$ is any point on the outer surface of cell number 3. The response due to a second neutron source was also computed in the adjoint calculation for illustration. This second source was

$$S(\underline{r}_s, E, \underline{\Omega}) = \frac{1}{4\pi} \frac{1}{6 \text{ MeV}} \frac{1}{4\pi |\underline{r}_s|^2} \text{ for } 6 \text{ MeV} < E < 12 \text{ MeV},$$

$$= 0 \text{ otherwise.}$$

Functional:

Number of first-generation fission neutrons produced in the ^{235}U.

The geometry is simple; i.e., there is spherical symmetry of both the extraneous source and the three cells. We may therefore concentrate on the input required for the coupled sampling without becoming involved with geometric details. Those who may be unfamiliar with the geometric capabilities of the MCN and MCNA codes are referred to Refs. 4, 5, and 6.

The sampling from the transport equation for this example problem was set up so that an estimate of the functional due to the 12- to 15-MeV neutron source was obtained while the functions for sampling from the adjoint equation were computed. This then provides one check between the adjoint and transport calculations. Thus, additional adjoint calculations can be made, with smaller ^{235}U cell radii for example, with confidence that the adjoint sampling has been set up correctly. This type of procedure has also been found advantageous for problems involving a given system response as a function of the neutron source distribution in space and energy. Adjoint problems of this type have been solved using hundreds of neutron source distributions, but a check on one of these distributions in the transport portion of the calculation is time well spent.

The neutron source in the Monte Carlo calculations was biased so that the source neutrons would always reach cell two. The neutron source is constructed in the same manner as in the MCN code.[4-6] Subroutine SOURCE for selecting the initial neutron parameters is shown in Fig. 4.

The pseudoneutron source was constructed from the built-in routines in MCNA. The initial position of the pseudoneutron was selected from a uniform distribution within the cell containing ^{235}U. A uniform selection is adequate at energies such that the number of mean free paths across the cell is small. However, at energies such that the number of mean free paths is large, most of the fission neutrons are born near the outer surface. This means that one may expect to gain efficiency in the adjoint calculation by biasing the selection of the pseudoneutrons at these energies toward the outer boundary. (This type of problem often occurs near thermal energies, where the fission cross section is large.) The biasing is accomplished in the example problem by calling the subroutine ASOURC after the built-in routines have been used to select the

```
      SUBROUTINE SCURCE
C
C     INTEGER, DIMENSION, CCMMCN, AND EQUIVALENCE STATEMENTS ARE NOT
C     SHOWN, BUT CCRRESPCND TO THOSE OF THE MAIN PROGRAM ATMC
C
C     BIASED NEUTRCN SOURCE TO STRIKE INNER SPHERE OF 16.51 CM DIAMETER
C     SRC(1)=R3 ,    SRC(2) = SQRT(1 - R2**2/R3**2)
C     SRC(3)=JA , SRC(4)=IA , SRC(5),SRC(6) ARE LOWER ENERGY AND ENERGY
C     SOURCE WIDTH
C
      X=-SRC(1)+.001  $  Y=0.  $  Z=0.  $  TME=0.  $ DEL=0.
      RN=FRN(R)
      U=SRC(2) + (1.-SRC(2))*RN  $  V=0.  $  W=SQRT(1.-U**2)
      ERG=SRC(5) + FRN(R)*SRC(6)
      JA=SRC(3)  $  IA=SRC(4)
      WT=(1.-SRC(2))/2.
      RETURN
      END
```

Fig. 4. Subroutine SOURCE to select the initial neutron parameters.

initial parameters (the 6th data entry of cards ASC = 1). In ASOURC, the product of the macroscopic fission cross section and the radius of the uranium region is computed. If this number is less than four, a return is made to the main program and the parameters selected by the built-in routines are accepted. If the number is greater than four, the initial distance r of the pseudoneutron from the center of the ^{235}U is selected from the density function

$$g(r) = e^{+\Sigma_f r} / \int_0^{r_u} e^{+\Sigma_f r'} \, dr' \quad , \qquad (42)$$

where Σ_f is the macroscopic fission cross section

and r_u is the radius of the uranium region. The radius, r, is obtained with a random number ξ as

$$r = r_u + \ln\left[1 - \xi\left(1 - e^{-\Sigma_f r_u}\right)\right] \Big/ \Sigma_f \quad , \qquad (43)$$

and the weight of pseudonuetron, as obtained by a uniform sampling, is multiplied by the ratio

$$\frac{4\pi r^2}{\frac{4}{3}\pi r_u^3 \, g(r)} = \frac{3r^2}{r_u^3} \frac{\left(1 - e^{-\Sigma_f r_u}\right)}{\Sigma_f \, e^{-\Sigma_f(r_u - r)}} \qquad (44)$$

The subroutine ASOURC for this example problem is given in Fig. 5. This subroutine is written for the more general case when the inner radius may not be zero. Here T1 is the inner radius, T11 is the

```
      SLBROUTINE ASOURC(APSC,T1,T11,XD,YD,ZD)
C
C     INTEGER, DIMENSION, CCMMC·I, AND EGUIVALENCE STATEMENTS ARE NOT
C     SHOWN, BUT CCRRESPCND TO THOSE OF THE MAIN PROGRAM ATMC
C
C     ADJUST THE SPATIAL POSITION CF THE SOURCE PSEUDO-NEUTRON WHEN
C     THE FISSION CROSS SECTICN APSC IS LARGE
C     T1  =  INNER RADIUS
C     T11 = OUTER RADIUS
      APSC=APSC*RHC(IA)/2.43
      IF(APSC*(T11-T1) . LT. 4.) RETURN
      PSC=APSC/(1.-EXP(-APSC*(T11-T1)))
      RAD=T11+ALCG(1.-APSC*FRN(R)/PSC)/APSC
      WT=WT*3.*RAD**2/((T11**3-T1**3)*PSC*EXP(-APSC*(T11-RAD)))
      X=RAD*U+XD  $  Y=RAD*V+YD  $  Z=RAD*W+ZD
C     SELECT NEW CIRECTICN ISOTROPICALLY
      U=1.-2.*FRN(R)
20931 TP(1)=1.-2.*FRN(R)  $  TP(2)=1.-2.*FRN(R)  $  TP(3)=TP(1)**2+TP(2)**2
      IF(TP(3).GT.1.) GO TO 20931  $  TP(4)=SQRT((1.-U**2)/TP(3))
      V=TP(1)*TP(4)  $  W=TP(2)*TP(4)
      RETURN
      END
```

Fig. 5. Subroutine ASOURC to alter the initial pseudoneutron position for large fission cross sections.

outer radius, APSC is ν times the microscopic fission cross section, and RHO is the density in atoms/barn-cm of ^{235}U; XD, YD, and ZD are zero in this problem. The last few cards select the direction of flight from an isotropic distribution.

The last routine required is subroutine SCORE for tabulating the functionals, the number of first-generation fission neutrons produced. Subroutine SCORE is shown in Fig. 6. In this case, two functionals are computed for illustration. The functional denoted by JC = 2 is the main functional of interest, i.e., the number of first-generation neutrons produced by a 12- to 15-MeV extraneous neutron source of unit strength. The functional denoted by JC = 1 is the number of first-generation fission neutrons produced by a 6- to 12-MeV extraneous neutron source of unit strength.

The appropriate score for these two functionals, each time a pseudoneutron crosses the outer surface, is obtained from Eq. (39a) as

$$\frac{\overline{W}}{4\pi} \frac{1}{(6 \text{ MeV})} \frac{1}{4\pi(30.5 \text{ cm})^2} \frac{1}{\mu_n} \text{, for } 6 \text{ MeV} < E < 12 \text{ MeV,}$$

(45)

$$\frac{\overline{W}}{4\pi} \frac{1}{3 \text{ MeV}} \frac{1}{4\pi(30.5 \text{ cm})^2} \frac{1}{\mu_n} \text{, for } 12 \text{ MeV} < E < 15 \text{ MeV.}$$

(46)

In subroutine SCORE of Fig. 6, the variable AJCON(1,1)

is 1/6 and the variable AJCON(2,1) is 1/3; these variables are a portion of the input data and will be mentioned later. The $1/(4\pi \ 30.5 \text{ cm})^2$ is lumped into the initial pseudoneutron weight because it is simply a constant. The variable UPRIM in Fig. 6 is the cosine of the angle, μ_n, between the direction of motion of the pseudoneutron and a vector normal to the surface. μ_n will never be close to zero, owing to the geometry of this problem, so the possibility of an infinite variance, as discussed in Sec. III for an isotropic source, will not occur.

The control cards and card input data for the CDC 6600 run are as shown in Fig. 7. The first few cards are control cards. Before discussing the input data for the coupled sampling, we will consider the magnetic tapes required to run MCNA.

Two magnetic tapes, CODETP and RUNTP, are used. CODETP contains the following five files.

File 1 -- The symbolic form of the MCNA program in UPDATE format.

File 2 -- Binary deck of ATMC (see Fig. 1, steps 3 and 5) and related subroutines.

File 3 -- Binary deck of ANUI (see Fig. 1, steps 2 and 4) and related subroutines.

File 4 -- Binary deck of ATTMC (see Fig. 1, step 1).

File 5 -- The MCNA cross-section library.

The general procedure for the use of CODETP is:

1. Using an old CODETP, make any necessary changes in Subroutines SOURCE, ASOURC, and SCORE and generate a new CODETP to include these changes.

```
      SUBROUTINE SCORE(KASR)
C
C     INTEGER, DIMENSION, COMMON, AND EQUIVALENCE STATEMENTS ARE NOT
C     SHOWN, BUT CORRESPOND TO THOSE OF THE MAIN PROGRAM ATMC
C
C     COMPUTE CONTRIBUTION OF PSEUDO-NEUTRON TO FIRST GENERATION
C     NEUTRONS
C
      IF(KASR.NE.2) GO TO 29
      IF(ERG.LT.6.) GO TO 29
      IF(ERG.GT.15.) GO TO 29
      IF(JA.NE.3) GO TO 29
      UPRIM = (U*X + V*Y + W*Z)/30.48
      JC=1
      IF(ERG.GT.12.) JC=2
      WCON=WT*AJCON(JC,1)/UPRIM
      TSCOR(JC)=TSCOR(JC)+WCON
   29 RETURN
      END
```

Fig. 6. Subroutine SCORE to compute the contribution of the pseudoneutron history to the first-generation source of fission neutrons.

```
ASSIGN MT,CODETP(NLB,LG918LOO,SHH)
ASSIGN MT,RUNTP(NLB,LI939LOO,SHH)
COPYBF(CODETP,DISCARD)
COPYBF(CODETP,D3)
REWIND(D3)
COPYBF(D3,RUNTP)
COPYBF(CODETP,ANLI)
COPYBF(CODEIP,AITMC)
AITMC.
COPYBF(RUNTP,DISCARD)
RFL,277000.
ANUI.
COPYBF(RUNTP,ATMC)
RFL,320000.
ATMC.
COPYBF(RUNTP,DISCARD)
RFL,277000.
ANUI.
7
    TEST CASE FOR GENERATING FIRST GENERATION FISSION SOURCE
        1  41  .0478  -1,2
        2  42  .1185  -2,3  1,1
        3  0   -3,4   2,2
        4  0   3,3

        1  S0  .635
        2  S0  8.255
        3  S0  30.48

    Y6  0  2R  0
    IO  1.  1.  1.  0.
    DO  .5E-6  0.  15.
    RO  1.E8
    R1  0.  2.5E-8  0.  0.
    M41  923  1.
    M42  11  .666667  3006  .333333
    S7  30.48  .9626  1  3  12.  3.

7
TYP   -1,1,1
ASC   3,0,2,1,1,1
ASP   0.,0.,0.,0.,C.,0.,C.,0.,C.,0.,0.,0.
ASI   -1,2,17,.91E7-4,0.,1.,1.
ST  1  0.        2.5-9    1.25-8   2.5-8    3.75-8   6.25-8   1.-7     1.5-7
       2.-7      3.-7     5.-7     3.06-6   2.26-5   .000167  .00123   .00912
       .0248     .0674    .183     .498     .821     1.35     2.23     2.87
       3.68      4.72     6.07     7.79     10.      12.      13.5     15.
       0.        .006     .038     .095     .134     .204     .268     .312
       .337      .369     .4       .42      .44      .47      .5       .514
       .524      .533     .559     .605     .65      .67      .695     .706
       .715      .727     .736     .752     .777     .8       .852     1.
AF  6
MN  1  0,0,0,0,0,1,1,1,1,1
AE  0  31,15.
AE  1  2.5-9    .041  .959  9.  5.
AE  2  1.25-8   .041  .959  9.  5.
AE  3  2.5-8    .041  .959  9.  5.
AE  4  3.75-8   .041  .959  9.  5.
AE  5  6.25-8   .041  .959  9.  5.
AE  6  1.-7     .041  .959  9.  5.
AE  7  1.5-7    .041  .959  9.  5.
AE  8  2.-7     .041  .959  9.  5.

AE  9  3.-7     .041  .959  9.  5.
AE 10  5.-7     .041  .959  9.  5.
AE 11  3.059-6  .041  .959  9.  5.
AE 12  2.26-5   .041  .959  9.  5.
```

Fig. 7. Control cards and input data for the example problem.   (cont.)

```
AE  13  .C0015/  .041  .959  9.    5.
AE  14  .0C123   .041  .959  9.    5.
AE  15  .00912   .041  .959  9.    5.
AE  16  .0248    .041  .959  9.    5.
AE  17  .0674    .476  .5    1.5  3.5  6.   3.
AE  18  .183     .433  .5    1.5  3.5  6.   3.
AE  19  .498     .317  .5    1.5  3.5  6.   3.
AE  20  .821     .5C2  1.5   2.5  4.   3.   3.
AE  21  1.35     .68   1.    2.5  4.   3.   3.
AE  22  2.23     1.15  2.5   4.   3.   3.
AE  23  2.87     1.27  2.5   3.5  2.5  3.
AF  24  3.68     1.13  2.    3.5  2.5  3.
A2  25  4.72     1.32  3.    3.5  2.   1.5
AE  26  6.07     2.28  2.5   2.5  1.5  1.5
AL  27  7.79     1.93  2.    2.   2.   1.
AE  28  10.      2.21  2.    2.   1.
AE  29  12.      1.5   1.5   1.   1.
AL  30  13.5     1.    1.    .5   .5
AE  31  15.      1.    .5
SCC   0,0,-1,-1                                                END DATA
7
  1.    +08  1.    -C8  10.        10000   500000        2    500000
7
TYP   2,1,3

7                                                                +++++



ASSIGN  MT,C IDETP(NLB,LG918L00,SHB)
ASSIGN  MT,RUNTP(NLB,LI939L00,SHB)
COPYBF(CODETP,DISCARD,2)
CJPYBF(CODETP,ANLI)
COPYBF(RUNTP,DISCARD)
ANLI.
COPYBF(RUNTP,ATMC)
RFL,32C0C0.
ATMC.
7
TYP   4,1,4
AF  1  .16666666666667
AF  2  .33333333333333
ALE 1  1.L-6  6.   3

7
 -1.    +08  1.    -15 5.2       100C0   500000        5    500000
7                                                                ++++++
```

Fig. 7 (continued)

The necessary control cards for doing this with the UPDATE program are shown in Fig. 8

2. Write the second file of the new CODETP onto the first file of RUNTP and use the other files as needed. This is illustrated in the control cards of Fig. 7.

3. Skip to the cross-section library before running AITMC.

The first file of RUNTP contains the program ATMC. This has been found convenient, and generally saves some tape handling. However, it does require that one skip past this record before execution of each program. The subsequent records of RUNTP, on the second file, are generated during the problem. These records are:

Record Number	Comment
1	Tape dump after initiation; Step 1 of Fig. 1.
2	Tape dump after Step 2 of Fig. 1.
3-n	Tape dumps during Step 3 of Fig. 1.
n+1	Tape dump after Step 4 of Fig. 1. Occasionally there will be another tape dump here (usually signified by a 3 or 4 in the first entry of card TYP, as described in Appendix B).
n+2 to m	Tape dumps during Step 5 of Fig. 1.

```
ASSIGN MT,OLDPL(NLB,LB247L00,SH8)
ASSIGN MT,CODETP(NLB,LG918L00,SH8)
UPDATE(N=CODETP)
RUN(S,,,COMPILE)
REWIND(LGO)
REWIND(OLDPL)
REWIND(CODETP)
COPYBF(OLDPL,DISCARD)
COPYBF(OLDPL,NEW1)
COPYBF(OLDPL,NEW2)
COPYBF(OLDPL,NEW3)
COPYBF(OLDPL,NEW4)
REWIND(NEW1)
REWIND(NEW2)
REWIND(NEW3)
REWIND(NEW4)
COPYBF(CODETP,DISCARD)
COPYBR(NEW1,DISCARD,7)
COPYBF(LGO,NEW1)
REWIND(NEW1)
COPYBF(NEW1,CODETP)
COPYBF(NEW2,CODETP)
COPYBF(NEW3,CODETP)
COPYBF(NEW4,CODETP)
7
CC     UPDATE CORRECTIONS GO HERE
7
```

Fig. 8. *Control cards required to utilize the
UPDATE program to alter subroutine SOURCE,
ASOURC, or SCORE.*

After some file manipulation, the program
AITMC is called by the ninth control card of Fig.
7. The input data, between the first and second
7-8-9 cards, for AITMC are identical to that for the
initiation of the MCN program and so are not dis-
cussed here. The AITMC program initiates the data,
selects the pertinent cross sections from the fifth
file of CODETP, and writes the blank common block
onto the first record of the second file of RUNTP.

The program ANUI is called by the 12th control
card of Fig. 7 (the MCNA program now uses ECS so
that the RFL memory allocation is normally less than
156K) and initiates the input data for the coupled
sampling between the second and third 7-8-9 cards;
see Appendix B for a description of the input data.
The following comments on the input data for this
example problem may be useful:

1. The second data entry on card TYP is 1, in-
dicating that only the first generation is consid-
ered. For most neutron multiplication problems,
this entry would be 0.

2. The sixth data entry of card ASC is 1, so
the main program, ATMC, calls subroutine ASOURC
after generating the initial pseudoneutron source
parameters from the built-in routines.

3. The pseudoneutron energy selection table,

ST1, was obtained from previous calculations on this
type of problem. In many problems, it is worth-
while to change this table after the transport por-
tion of the calculation because useful information
is often obtained there.

4. The initial pseudoneutron weight is com-
puted from Eq. (38). Here $\bar{g}$ in the cell containing
^{235}U is given by

$$\bar{g}(\underline{r},E,\underline{\Omega}) = \frac{1}{\frac{4}{3}\pi r_u^3 \, 4\pi} \, g_E(E) \quad , \qquad (47)$$

where $g_E(E)$ is the energy spectrum as input on card
ST1. The code automatically multiplies the initial
weight constant, input as the fourth data entry on
card ASI, by $\nu\Sigma_f/g_E(E)$. The initial weight constant
for the fourth data entry is given by

$$\frac{\frac{4}{3}\pi r_u^3 \, 4\pi}{(4\pi \; 30.5 \; \text{cm})^2} = \frac{0.635^3 \; \text{cm}}{3 \times 30.5^2} = 0.9187 \times 10^{-4} \; \text{cm} , \quad (48)$$

where the factor $1/(4\pi \; 30.5 \; \text{cm})^2$ has been included.

5. The floating-point number at which the
pseudoneutron weight is split, as given by the sixth
data entry on card ASI, provides an opportunity for
splitting when large weights occur. It should ordi-
narily be set large enough so that splitting occurs
infrequently, one split per hundred source pseudo-
neutrons, for example.

6. A hydrogen transfer matrix is used in this
problem because of the large amount of leakage, but
this is usually unnecessary.

7. Six functionals are designated on the AF
card because the transport portion of the calcula-
tion was altered slightly to compute the number of
first-generation fission neutrons produced. Thus,
a check can be made between the adjoint and trans-
port calculations for one geometric configuration.

8. The adjoint calculations usually tend to be
insensitive to the energy mesh utilized on the AE
card. The infinite number of possibilities makes
this very difficult to optimize.

The program ATMC is called by the 15th control
card of Fig. 7 to begin the sampling from the trans-
port equation. The program ANUI is called again by
the 18th control card to normalize the sampling
functions. Additional input data are not required
at this stage, so only a TYP card is needed. How-
ever, after the normalization, the program ANUI is
called again (note that the last tape dump from the

previous calculation is used) and the number of functionals is also changed from six to two with the proper functional constants inserted. The special leakage option is also introduced here with the ALE card. Note that we could have made these changes in the previous step, but this illustrates the use of tape dumps at any point in the calculation.

The program ATMC is now called again for the final sampling from the adjoint equation. The printed output of the adjoint calculation is given in Fig. 9. The number of first-generation fission neutrons of 0.742×10^{-4} ($\pm$ 0.078), as computed by

TEST CASE FOR GENERATING FIRST-GENERATION FISSION SOURCE

SOURCE NO.	TIME CUTOFF	WEIGHT CUTOFF	RUN TIME	D.P. CYCLE	DUMP CYCLE	DUMP NO.	CUTOFF CYCLE
7	-1.0000E+08	1.0000E-15	5.2000E+00	10000	500000	5	500000

TEST CASE FOR GENERATING FIRST-GENERATION FISSION SOURCE

TIME = 5.003 MINUTES

NUMBER OF NEUTRONS STARTED	TOTAL NUMBER OF COLLISIONS	RANDOM NUMBERS GENERATED	TOTAL WEIGHT STARTED	TOTAL ENERGY STARTED	COLLISIONS PER NEUTRON STARTED	TRACKS PER NEUTRON STARTED	NEUTRONS PROCESSED PER MINUTE
21450	97290	917428	8.1714E+00	7.8982E+04	4.5357E+00	1.0001E+00	4.2878E+03

TOTAL TRACKS STARTED	LOSS TO ENERGY CUTOFF	LOSS TO TIME CUTOFF	LOSS TO WEIGHT CUTOFF	LOSS TO ESCAPE	LOSS TO SPLITTING	TOTAL TRACKS LOST
21452	2105	0	312	10984	8051	21452

WEIGHT STARTED PER NEUTRON	LOSS TO ENERGY CUTOFF	LOSS TO TIME CUTOFF	LOSS TO WEIGHT CUTOFF	LOSS TO ESCAPE	LOSS TO CAPTURE	WEIGHT LOST PER NEUTRON
3.8095E-04	2.8489E-05	0.	0.	1.7732E-03	-1.4766E-03	3.2506E-04

ENERGY STARTED PER NEUTRON	LOSS TO ENERGY CUTOFF	LOSS TO TIME CUTOFF	LOSS TO WEIGHT CUTOFF	LOSS TO ESCAPE	LOSS TO CAPTURE	
3.6821E +00	4.7522E-04	0.	0.	1.0364E-02	6.6719E-03	

TOTAL NUMBER OF EVENTS

ELASTIC	FISSION	INEL. C.M.	INEL. D.M.L.	INEL. D. M. C.	
85585	0	2170	1484	0	30886

FUNCTIONAL ESTIMATES OBTAINED BY SAMPLING FROM THE ADJOINT EQUATION

FUNCTIONAL NUMBER	FUNCTIONAL ESTIMATE	RELATIVE ERROR	VARIANCE RELIABILITY
1	.87540E-04	.11933E+00	.39626E+00
2	.74244E-04	.77714E-01	.52021E+00

****

TAPE DUMP NO. 6   NPS = 21450

****

Fig. 9. Printed output of the adjoint portion of
the calculation for the example problem.

the adjoint calculation, compares favorably to the transport result of $0.854 \times 10^{-4}(\pm 0.12)$. Here the errors quoted are relative errors (standard deviation divided by the functionals). These relative errors are large owing to the importance of leakage in this problem. The relative error of the functional due to the 12- to 15-MeV source could be reduced by a factor of ~ 0.8 in the adjoint calculation by extending the energy range to 12 MeV for sampling so that leakage would not occur; i.e., the third data entry of card ALE would be set to 12. instead of 6. This was not done here to illustrate the computation of the two functionals. An alternate approach for this example problem is to alter subroutine SCORE to tabulate the functionals only

when KASR is equal to 4, and to multiply the scoring by the leakage probability ANL. Then, with the third data entry of card ALE set to 15., both functionals could be tabulated and the leakage treated adequately.

For the nuclear safeguard problems, the program ATMC was altered so that different radii could be input for the ^{235}U cell and the moderator cell. A parameter study was then made for different radii by sampling from the adjoint equation and using the sampling scheme constructed in the one transport calculation. Of course, the adjoint solution is not limited to this simple geometry, which was an incentive for using the Monte Carlo method.

APPENDIX A

DENSITY FUNCTIONS AND WEIGHT FACTORS FOR SAMPLING FROM THE ADJOINT EQUATION

The computation of the $\overline{Q}_\alpha$'s and their subsequent use in the sampling from the adjoint equation were discussed in Sec. III. The corresponding $\overline{f}_\alpha$ density functions are discussed here, and the pseudo-neutron weight following each type of event α is derived. The four α events are considered in the same sequence as in Sec. III.

1. Elastic Scattering with an Isotope

a. *Epithermal Elastic Scattering.* A superscript i denotes that the elastic scattering event is with isotope i. Σ_1^i is the macroscopic elastic scattering cross section of isotope i, C_1^i is the collision kernel, and $\overline{f}_1^i$ is the corresponding density function to sample the energy and direction of motion. It is convenient (assuming isotropic media) to expand each density function into the product of a marginal density function for the laboratory scattering angle μ_L and a conditional density function (a Dirac delta function for the energy). The relevant expansions are

$$C_1^i(E', -\underline{\Omega}_a'; \underline{r}, E, -\underline{\Omega}_a)$$

$$= \frac{1}{2\pi} D_1^i(\mu_L; \underline{r}, E)_L \delta \left\{ E' - \frac{E\left[(1-\overline{\alpha})\mu_{cm} + 1 + \overline{\alpha}\right]}{2} \right\}_{E'}, \quad \text{(A.1)}$$

$$\overline{f}_1^i(E, \underline{\Omega}_a; \underline{r}, E', \underline{\Omega}_a')$$

$$= \frac{1}{2\pi} h_1^i(\mu_L; \underline{r}, E')_L \delta \left\{ E - \frac{2E'}{\left[(1-\overline{\alpha})\mu_{cm} + 1 + \overline{\alpha}\right]} \right\}_E, \quad \text{(A.2)}$$

where

$$\overline{\alpha} = \left(\frac{A-1}{A+1} \right)^2, \quad \text{(A.3)}$$

μ_{cm} is the scattering angle in the center-of-mass system, and the subscripts E' and E on the delta functions serve as a reminder that they are normalized as

$$\int \delta \left\{ E' - \frac{E\left[(1-\overline{\alpha})\mu_{cm} + 1 + \overline{\alpha}\right]}{2} \right\}_{E'} dE' = 1, \quad \text{(A.4)}$$

$$\int \delta \left\{ E - \frac{2E'}{\left[(1-\overline{\alpha})\mu_{cm} + 1 + \overline{\alpha}\right]} \right\}_E dE = 1. \quad \text{(A.5)}$$

A transformation to the center-of-mass system is useful as

$$D_1^i(\mu_{cm};\underline{r},E)_{cm} = D_1^i(\mu_L;\underline{r},E)_L \frac{\partial \mu_L}{\partial \mu_{cm}} \quad , \qquad (A.6)$$

$$h_1^i(\mu_{cm};\underline{r},E)_{cm} = h_1^i(\mu_L;\underline{r},E')_L \frac{\partial \mu_L}{\partial \mu_{cm}} \quad , \qquad (A.7)$$

where the subscripts cm and L on D_1^i and h_1^i denote density functions in the center-of-mass and laboratory systems, respectively. The density function h_1^i of Eq. (A.7) may now be specified, and in MCNA it is chosen to be

$$h_1^i(\mu_{cm};\underline{r},E')_{cm} = D_1^i\left[\mu_{cm};\underline{r}, \frac{E'}{2}\left(1 + \frac{1}{\bar{\alpha}}\right)\right]_{cm} . \qquad (A.8)$$

This density function is easy to sample and has some other useful properties. It is the exact zero-variance density function in regions of phase space where the neutron flux is isotropic, $\varphi(\underline{r},E)\Sigma_1^i(\underline{r},E)$ is inversely proportional to E, and $D_1^i(\mu_{cm};\underline{r},E)_{cm}$ does not change for $E' \le E \le E'/\bar{\alpha}$. Although these conditions are seldom met exactly, this approximation is expected to be adequate for most problems.

After the center-of-mass scattering angle μ_{cm} is selected and the energy E is computed, the pseudo-neutron weight is obtained from Eqs. (24), (A.1), (A.2), (A.6), (A.7), and (A.8) as

$$\overline{W} = \frac{\overline{W}' C_1^i(E', -\underline{\Omega}_a';\underline{r},E, -\underline{\Omega}_a)\Sigma_1^i(\underline{r},E)}{\Sigma_t(\underline{r},E')\overline{Q}_1(j,k,i)\overline{P}_1^i(E,\underline{\Omega}_a;\underline{r},E',\underline{\Omega}_a')} \qquad (A.9)$$

$$= \frac{\overline{W}'\Sigma_1^i(\underline{r},E)D(\mu_{cm};\underline{r},E)_{cm}}{\Sigma_t(\underline{r},E')\overline{Q}_1(j,k,i)D\left[\mu_{cm};\underline{r}, \frac{E'}{2}\left(1 + \frac{1}{\bar{\alpha}}\right)\right]_{cm}} \frac{E}{E'} \quad ,$$

where the factor E/E' arises owing to the ratio of the delta functions,

$$\frac{\delta\left\{E' - \frac{E\left[(1 - \bar{\alpha})\mu_{cm} + 1 + \bar{\alpha}\right]}{2}\right\}_{E'}}{\delta\left\{E - \frac{2E'}{\left[(1 - \bar{\alpha})\mu_{cm} + 1 + \bar{\alpha}\right]}\right\}_E} = \frac{dE}{dE'} = \frac{E}{E'} \quad . \quad (A.10)$$

A special option for hydrogen is available for choosing a density function other than $h_1^i(\mu_{cm};\underline{r},E)_{cm}$ of Eq. (A.8). With this option, the sampling from the transport equation is used to compute the number

of neutrons in energy group γ that suffer a scattering collision with hydrogen in cell k and are transferred to energy group j. In the subsequent sampling from the adjoint equation, each time a pseudo-neutron suffers a collision with hydrogen in energy group j and cell k, the postcollision energy group γ is selected with a probability proportional to the number of neutrons that scattered with hydrogen and were transferred from γ to j. The pseudoneutron energy E within group γ is selected from a density function proportional to $1/E^2$ and the pseudoneutron weight computed as

$$\overline{W} = \frac{\overline{W}'\Sigma_1^i(\underline{r},E)D_1^i(\mu_{cm};\underline{r},E)_{cm}}{\Sigma_t(r,E')\overline{Q}_1(j,k,i)\beta(j,k,\gamma)} \left[\frac{1}{\left(E_L\right)_\gamma} - \frac{1}{\left(E_u\right)_\gamma}\right] 2E \quad ,$$

$$(A.11)$$

where $\beta(j,k,\gamma)$ is the probability of selecting energy group γ, $(E_L)_\gamma$ is the lower boundary of group γ, and $(E_u)_\gamma$ is the upper boundary of group γ.

b. _Thermal Elastic Scattering._ The MCNA code uses the same simple scattering models as the MCN code for energies below a thermal upper bound designated by the quantity (EBR) in the code; i.e., the laboratory angle is selected isotropically and the energy remains unchanged for neutron collisions with nuclei of mass A > 2, and the free-gas model is used for hydrogen and deuterium.

The free-gas model is used in the MCNA code by sampling from the neutron transport equation to construct a thermal transfer matrix for each cell containing hydrogen or deuterium (two transfer matrices for a cell containing both). Let isotope i be either hydrogen or deuterium and assumed to be in region k and let the transfer matrix be $T(j,j')_{ik}$. Then the matrix $T(j,j')_{ik}$ is computed in the sampling from the transport equation as

$$T(j,j')_{ik} = \frac{\begin{array}{l}\text{Number of neutrons suffering a}\\\text{collision with isotope i in en-}\\\text{ergy group } j' \text{ and cell k that}\\\text{emerge from the collision in}\\\text{thermal energy group } j.\end{array}}{\text{Sum of the numerator over all } j'} \quad .$$

$$(A.12)$$

Ten thermal groups* must be used in MCNA, so j assumes values from 1 to 10 and j' from 1 to 11 (in

_____
*See input card AEQ of Appendix B for the thermal group boundaries.

this discussion of thermal scattering, all epithermal energies are denoted by energy group 11). In the subsequent sampling from the adjoint equation, the new energy group j' of the pseudoneutron, after suffering a collision with isotope i in thermal energy group j, is randomly selected from the probabilities

$$T(j,j')_{ik} \quad , \quad 1 \leq j' \leq 11 \quad . \quad (A.13)$$

The final energy E of the pseudoneutron within group $j'(j' \neq 11)$ is then selected with density function

from a density function inversely proportional to E^2.

Eqs. (A.12) to (A.15) are derived for the free-gas model with $A \leq 2$. We will now consider $A > 2$. Given that $A > 2$ and that the precollision energy of the pseudoneutron is less than $(EBR)*\bar{\alpha}$, the pseudoneutron energy remains unchanged at the elastic collision, the new direction of flight is selected from an isotropic distribution, and the pseudoneutron weight is obtained as

$$b_1^i(E,\underline{\Omega}_a;\underline{r},E',\underline{\Omega}_a') = \frac{\Sigma_1^i(\underline{r},E)C_1^i(E', -\underline{\Omega}_a';\underline{r},E, -\underline{\Omega}_a)\Phi(E)_{j'}}{\int_{\Omega''}\int_{(E_L)_{j'}}^{(E_u)_{j'}} \Sigma_1^i(\underline{r},E'')C_1^i(E', -\underline{\Omega}_a';\underline{r},E'', -\underline{\Omega}_a'')\Phi(E'')_{j'}dE'' \, d\underline{\Omega}_a''} \quad \text{for} \quad (E_L)_{j'} < E < (E_u)_{j'} \quad , $$

$$(A.14)$$

where the user may specify $\Phi(E)_{j'}$ within group j' to be either proportional to a Maxwellian flux $Ee^{-E/T}$ or inversely proportional to E. In Eq. (A.14), $\Sigma_1^i(\underline{r},E)C_1^i(E', -\underline{\Omega}_a';\underline{r},E, -\underline{\Omega}_a)$ is the free-gas scattering kernel; see Eq. (2.19) of Williams.[14] This scattering kernel is a function of the temperature T in the medium, but that dependence has been suppressed here for compact notation. An option is also available in MCNA to allow the temperature T to change with time, as in the MCN code.

The pseudoneutron weight after the collision with isotope i (hydrogen or deuterium) is obtained from Eqs. (24) and (A.14) as

$$\bar{W} = \frac{\bar{W}\Sigma_1^i(\underline{r},E')}{\Sigma_t(\underline{r},E')\bar{Q}_1(j,k,i)} \quad . \quad (A.16)$$

If the precollision energy of the pseudoneutron is less than (EBR) but greater than $(EBR)\bar{\alpha}$, with probability

$$\gamma = \frac{\dfrac{1}{E'} - \dfrac{1}{(EBR)}}{\dfrac{1}{E'} - \dfrac{\bar{\alpha}}{E'}} \quad , \quad (A.17)$$

the energy does not change at the elastic collision, the new direction is sampled isotropically in the

$$\bar{W} = \frac{\bar{W}'\Sigma_1^i(\underline{r},E)C_1^i(E', -\underline{\Omega}_a';\underline{r},E, -\underline{\Omega}_a)}{\Sigma_t(\underline{r},E')\bar{Q}_1(j,k,i)T(j,j')_{ik} \, b_1^i(E,\underline{\Omega}_a;\underline{r},E,\underline{\Omega}_a')}$$

$$(A.15)$$

$$= \frac{\bar{W}'\int_{\Omega''}\int_{(E_L)_{j''}}^{(E_u)_{j''}} \Sigma_1^i(\underline{r},E'')C_1^i(E', -\underline{\Omega}_a';\underline{r},E'', -\underline{\Omega}_a'')\Phi(E'')_j dE'' \, d\underline{\Omega}_a''}{\Sigma_t(\underline{r},E')\bar{Q}_1(j,k,i)T(j,j')_{ik}\Phi(E)_{j'}} \quad .$$

If the pseudoneutron scatters to an epithermal energy ($j' = 11$), the density function C_i is taken from the tabulated values in the cross-section library and the energy of the pseudoneutron is selected

laboratory system, and the weight is given by the right-hand side of Eq. (A.16) except that the probability γ is inserted in the denominator. With probability $(1 - \gamma)$, the center-of-mass scattering

angle is selected from a uniform distribution between the limits

$$- 1 \quad \text{and} \quad \frac{2E'}{(1 - \bar{\alpha})(EBR)} - \frac{(1 + \bar{\alpha})}{(1 - \bar{\alpha})} \quad ,$$

the energy E of the pseudoneutron after the collision is

$$E = \frac{2E'}{(1 - \bar{\alpha})\mu_{cm} + 1 + \bar{\alpha}} \quad , \qquad (A.18)$$

and the weight is obtained as

$$\bar{W} = \frac{\bar{W}' \, \Sigma_1^i(\underline{r},E)D(\mu_{cm};\underline{r},E)}{\Sigma_t(\underline{r},E')\bar{Q}_1(j,k,i)} \frac{2E}{E'} \quad . \qquad (A.19)$$

2. Inelastic Scattering with a Continuum Density Function

The random selection of a $\bar{Q}_2(j,k,\beta)$ probability restricts the final pseudoneutron energy to the segment from

$$E' + \sum_{\beta'=1}^{\beta-1} \Delta E_{\beta'} \quad \text{to} \quad E' + \sum_{\beta'=1}^{\beta} \Delta E_{\beta'} \quad , \qquad (A.20)$$

where $\Delta E_{\beta'}$ is the width of the inelastic energy band β'. The density function within this band may be chosen to be constant, and the energy E may be selected as

$$E = E' + \sum_{\beta'=1}^{\beta-1} \Delta E_{\beta'} + \Delta E_\beta \xi \quad , \qquad (A.21)$$

where ξ is a random number on the unit interval. The new direction of motion is selected from an isotropic distribution in the laboratory system, and the pseudoneutron weight is obtained from Eq. (24) as

$$\bar{W} = \frac{\bar{W}' \displaystyle\sum_i \Sigma_2^i(\underline{r},E)c_2^i\big(E,\mu_L;\underline{r},E, - \underline{\Omega}_a\big)_L 4\pi\Delta E_\beta}{\Sigma_t(\underline{r},E')\bar{Q}_2(j,k,\beta)} \quad , \quad (A.22)$$

where the subscript 2 denotes inelastic scattering with a continuous-type energy transfer density function and the superscript i is again used to designate isotope i. The L subscript on c_2^i is a reminder that this density function is in the laboratory system and the μ_L is used in c_2^i rather than $-\underline{\Omega}_a'$ for convenience (the physical model assumes that

the density function depends only on $- \underline{\Omega}_a \cdot - \underline{\Omega}_a' = \mu_L$). However, this density function is sometimes tabulated in the center-of-mass system. If the center-of-mass density function is denoted by $c_2^i(E',\mu_{cm};\underline{r},E, - \underline{\Omega}_a)_{cm}$, the corresponding density function in the laboratory system may be obtained by the transformation

$$c_2^i(E',\mu_L;\underline{r},E, - \underline{\Omega}_a)_L = c_2^i(E'_{cm},\mu_{cm};\underline{r},E, - \underline{\Omega}_a)_{cm}|J| \; ,$$

$$(A.23)$$

where J is the Jacobian,[15]

$$|J| = \begin{vmatrix} \dfrac{\partial E'_{cm}}{\partial E'} & \dfrac{\partial \mu_{cm}}{\partial E'} \\[3mm] \dfrac{\partial E'_{cm}}{\partial \mu_L} & \dfrac{\partial \mu_{cm}}{\partial \mu_L} \end{vmatrix} \quad , \qquad (A.24)$$

and the variables in the transformation are related as

$$E' = E'_{cm} + \Big[E + 2\mu_{cm}(A + 1)\sqrt{EE'_{cm}}\Big]\Big/(A + 1)^2 \quad ,$$

$$(A.25)$$

$$\mu_L = \mu_{cm}\sqrt{\frac{E'_{cm}}{E'}} + \sqrt{\frac{E}{E'}}\frac{1}{A + 1} \quad . \qquad (A.26)$$

Equations (A.25) and (A.26) may be used to obtain the relationships

$$E'_{cm} = E' + \frac{E}{(A + 1)^2} - \frac{2\mu_L\sqrt{EE'}}{(A + 1)} \quad , \qquad (A.27)$$

$$\mu_{cm} = \frac{\mu_L - \sqrt{\dfrac{E}{E'}}\dfrac{1}{(A + 1)}}{\Big[1 + \dfrac{E}{E'(A + 1)^2} - \dfrac{2\mu_L}{(A + 1)}\sqrt{\dfrac{E}{E'}}\Big]^{1/2}} \quad , \quad (A.28)$$

$$\frac{\partial E'_{cm}}{\partial E'} = 1 - \frac{\mu_L}{A + 1}\sqrt{\frac{E}{E'}}$$

$$= \frac{1}{2} + \frac{E'_{cm}}{2E'} - \frac{1}{2}\frac{E}{E'}\frac{1}{(A + 1)^2} \quad , \qquad (A.29)$$

$$\frac{\partial E'_{cm}}{\partial \mu_L} = - \frac{2\sqrt{EE'}}{A + 1} \qquad (A.30)$$

$$\frac{\partial \mu_{cm}}{\partial \mu_L} = \sqrt{\frac{E'}{E'_{cm}}} + \left(\frac{E'}{E'_{cm}}\right)^{3/2}\left(\mu_L - \sqrt{\frac{E}{E'}}\frac{1}{A+1}\right)\frac{1}{A+1}\sqrt{\frac{E}{E'}}$$

$$= \frac{E'}{E'_{cm}} + \frac{\sqrt{EE'}}{E'_{cm}}\frac{\mu_{cm}}{A+1} \quad , \tag{A.31}$$

energy dE' about E' by an event of type 2 is nearly independent of E. This is not usually true if the function

$$\sum_i \Sigma_2^i(\underline{r},E)c_2^i(E',\mu_L;\underline{r},E, -\underline{\Omega}_a)_L \tag{A.34}$$

$$\frac{\partial \mu_{cm}}{\partial E'} = \frac{1}{2}\sqrt{\frac{E}{E'_{cm}}}\,\frac{1}{E'(A+1)} - \frac{1}{2}\left(\frac{E'}{E'_{cm}}\right)^{3/2}\left(\mu_L - \sqrt{\frac{E}{E'}}\frac{1}{A+1}\right)\left[-\frac{E}{(E')^2(A+1)^2} + \frac{\mu_L\sqrt{E}}{(A+1)(E')^{3/2}}\right]$$

$$= \frac{1}{2}\sqrt{\frac{E}{E'_{cm}}}\,\frac{1}{E'(A+1)} + \frac{1}{4}\frac{\mu_{cm}}{E'_{cm}E'}\left[E'_{cm} - E' + \frac{E}{(A+1)^2}\right] \quad , \tag{A.32}$$

and

$$|J| = \left| \frac{\partial E'_{cm}}{\partial E'}\frac{\partial \mu_{cm}}{\partial \mu_L} - \frac{\partial E'_{cm}}{\partial \mu_L}\frac{\partial \mu_{cm}}{\partial E'} \right|$$

$$= \left| \frac{1}{2}\sqrt{\frac{E'}{E'_{cm}}} + \frac{1}{2}\sqrt{\frac{E'_{cm}}{E'}} - \frac{1}{2}\frac{E}{\sqrt{E'_{cm}E'}}\frac{1}{(A+1)^2} + \mu_{cm}\left[\frac{\sqrt{EE'}}{2E'_{cm}}\frac{1}{A+1} + \frac{1}{2}\sqrt{\frac{E}{E'}}\frac{1}{A+1}\right. \right.$$

$$\left. - \frac{1}{2}\frac{E^{3/2}}{E'_{cm}\sqrt{E'}}\frac{1}{(A+1)^3}\right] + \frac{E}{\sqrt{E'_{cm}E'}}\frac{1}{(A+1)^2} + \mu_{cm}\left[\frac{1}{2}\sqrt{\frac{E}{E'}}\frac{1}{A+1} - \frac{1}{2}\frac{\sqrt{EE'}}{E'_{cm}}\frac{1}{A+1}\right.$$

$$\left.\left. + \frac{1}{2}\frac{(E)^{3/2}}{E'_{cm}\sqrt{E'}}\frac{1}{(A+1)^3}\right]\right|$$

$$= \left| \frac{1}{2}\sqrt{\frac{E'}{E'_{cm}}} + \frac{1}{2}\sqrt{\frac{E'_{cm}}{E'}} + \frac{1}{2}\frac{E}{\sqrt{E'_{cm}E'}}\frac{1}{(A+1)^2} + \mu_{cm}\sqrt{\frac{E}{E'}}\frac{1}{A+1} \right|$$

$$= \sqrt{\frac{E'}{E'_{cm}}} \quad , \tag{A.33}$$

which is the Jacobian required in Eq. (A.23).

A constant-density function was used in Eq. (A.21) to sample for the pseudoneutron energy E within an inelastic band ΔE_β. This is a reasonable approximation to the zero-variance density function, provided that the rate of transfer of neutrons from an energy E, $E' + \sum_{\beta'=1}^{\beta-1}\Delta E_{\beta'} \le E \le E' + \sum_{\beta'=1}^{\beta}\Delta E_{\beta'}$, to an changes rapidly over the permissible limits of E. A more optimal sampling may then be expected through sampling proportional to the function of Eq. (A.34). An option is available in MCNA to randomly select eight energies E_γ as

$$E_\gamma = E' + \sum_{\beta'=1}^{\beta=1}\Delta E_{\beta'} + \frac{\Delta E_\beta}{8}(\xi + \gamma - 1) \quad , \tag{A.35}$$

where ξ is a random number on the unit interval (the same random number is used in computing the eight energies).

The energy $E = E_\gamma$ of the pseudoneutron is randomly selected with probability

$$\frac{\sum_i \Sigma_2^i(\underline{r},E_\gamma)c_2^i(E',\mu_L;\underline{r},E_\gamma, -\underline{\Omega}_a)_L}{\sum_{\gamma'=1}^8 \sum_i \Sigma_2^i(\underline{r},E_{\gamma'})c_2^i(E',\mu_L;\underline{r},E_{\gamma'}, -\underline{\Omega}_a)_L} \quad . \quad (A.36)$$

The pseudoneutron weight is computed as

$$\overline{W} = \frac{\overline{W}' \sum_{\gamma'=1}^8 \sum_i \Sigma_2^i(\underline{r},E_{\gamma'})c_2^i(E',\mu_L;E_{\gamma'}, -\underline{\Omega}_a)_L \, 4\pi\Delta E_\beta}{\Sigma_t(\underline{r},E')\overline{Q}_2(j,k,8)8} \quad . \quad (A.37)$$

This method of selection tends to produce a smoother weight than that obtained from Eq. (A.22). The computational effort required to select the energy E is nearly a factor of 8 greater, but if some of the c_2^i's are rapidly varying functions, this additional computation time may be worthwhile. This method of selection should be necessary only for isotopes of large A and for energies E less than about 2 MeV. Hence, these events may be rare, and the additional time required may be negligible compared to the total computation time.

3. Inelastic Scattering with a Discrete Model

a. Laboratory System. A model used in the MCN and MCNA computer codes is that of an inelastic scattering reaction in which the neutron is assumed to lose a discrete amount of energy in the laboratory system. The postcollision neutron energy E' is related to the precollision neutron energy E in this model as

$$E' = (E - \epsilon)/\eta \quad , \quad (A.38)$$

where ϵ and η are constants at an energy E.

In sampling from the adjoint equation, E' is the precollision energy, and the postcollision energy E of the pseudoneutron is determined as

$$E = \eta E' + \epsilon \quad . \quad (A.39)$$

The new direction of flight is selected from an iso-

tropic distribution, and the pseudoneutron weight after the collision may be obtained from Eq. (24) as

$$\overline{W} = \frac{\overline{W}' \Sigma_3^i(\underline{r},E)_\ell c_3^i(E', -\underline{\Omega}'_a;\underline{r},E, -\underline{\Omega}_a)_\ell}{\Sigma_t(\underline{r},E')\overline{Q}_3(j,k,i,\ell)\delta(E - \eta E' - \epsilon)_E \frac{1}{4\pi}} =$$

$$= \frac{\overline{W}' \Sigma_3^i(\underline{r},E)_\ell \frac{1}{2\pi} D_3^i(\mu_L;\underline{r},E)_\ell \delta(E'-(E-\epsilon)/\eta)_E \, v_3^i(\underline{r},E)_\ell}{\Sigma_t(\underline{r},E')\overline{Q}_3(j,k,i,\ell)\delta(E - \eta E' - \epsilon)_E \frac{1}{4\pi}}$$

$$= \frac{\overline{W}' \Sigma_3^i(\underline{r},E)_\ell \, D_3^i(\mu_L;\underline{r},E)_\ell \, 2\eta v_3^i(\underline{r},E)_\ell}{\Sigma_t(\underline{r},E)\overline{Q}_3(j,k,i,\ell)} \quad , \quad (A.40)$$

where the subscript ℓ denotes the inelastic level, $D_3^i(\mu_L;\underline{r},E)_\ell$ is the density function for the cosine of the scattering angle μ_L, and $v_3^i(\underline{r},E)_\ell$ is the total number of neutrons that emerge from the reaction.

b. Center-of-Mass System. A model used in the MCN and MCNA computer codes is that of an inelastic scattering reaction with the neutron assumed to lose a discrete amount of energy in the center-of-mass system. The relevant equations for the neutron are

$$E = \eta E'_{cm} + \epsilon \quad , \quad (A.41)$$

$$E' = E'_{cm} + \left[E + 2\mu_{cm}(A+1)\sqrt{EE'_{cm}}\right]\Big/(A+1)^2 \quad , \quad (A.42)$$

$$\mu_L = \mu_{cm}\sqrt{\frac{E'_{cm}}{E'}} + \sqrt{\frac{E}{E'}}\left(\frac{1}{A+1}\right) \quad , \quad (A.43)$$

where E is the precollision neutron energy in the laboratory system, E' is the postcollision neutron energy in the laboratory system, and E'_{cm} is the postcollision neutron energy in the center-of-mass system. ϵ is the minimum neutron energy required to excite the level, and η is the constant

$$\eta = \left(\frac{A+1}{A}\right)^2 \quad . \quad (A.44)$$

The inelastic threshold ϵ depends upon the isotope and level, but for notational convenience these subscripts are suppressed.

The relevant collision kernel c_3^i may be expressed as the number of neutrons that emerge from the reaction $v_3^i(\underline{r},E)_\ell$ multiplied by a marginal

density function $P_3^i(E';\underline{r},E)$ for the energy E' and a conditional density function, a Dirac delta function, for the cosine of the scattering angle μ_L. If the scattering is assumed isotropic* in the center-of-mass system, the density function P_3^i is given by

$$P_3^i(E';\underline{r},E) = \frac{(A+1)^2}{4A} \; \frac{1}{E\sqrt{1-\frac{\epsilon}{E}}} \quad , \quad \frac{E\left(A\sqrt{1-\frac{\epsilon}{E}}-1\right)^2}{(A+1)^2} \le E' \le \frac{E\left(A\sqrt{1-\frac{\epsilon}{E}}+1\right)^2}{(A+1)^2} \quad ,$$

$$= 0 \text{ for all other } E'. \tag{A.45}$$

In the adjoint solution, E' is the precollision energy, and the problem is to choose a density function to select the postcollision energy E of the pseudoneutron. The first step is to determine the bounds of E for a given E'. The following results, Eqs. (A.46) to (A.51), are from a derivation by Kalos et al.[16] The energy E must fall between a lower bound $E^L(E')$ and an upper bound $E^u(E')$ given by

$$E^L(E') = \frac{\epsilon}{1-y(1)^2} \quad , \tag{A.46}$$

$$E^u(E') = \frac{\epsilon}{1-y(-1)^2} \quad , \tag{A.47}$$

where

$$y(1) = \frac{2a}{(1+\sqrt{1+4ab})} \quad , \tag{A.48}$$

$$y(-1) = (1+\sqrt{1+4ab})/2b \quad ,$$

$$= \frac{a}{by(1)} \quad , \tag{A.49}$$

$$a = \left[\frac{(A+1)^2 \, E'}{\epsilon} - 1\right]\bigg/ 2A \quad , \tag{A.50}$$

$$b = \left[\frac{(A+1)^2 \, E'}{\epsilon} + A^2\right]\bigg/ 2A \quad . \tag{A.51}$$

---

*This requirement will be removed later.

The energy width from $E^L(E')$ to $E^u(E')$ is usually narrow so that a reasonable assumption is that the product of the neutron flux and the cross section for this event is nearly constant over this energy width. With this assumption, the approximation to the zero-variance density function is

$$h_3^i(E;\underline{r},E') = \frac{P_3^i(E';\underline{r},E)}{\displaystyle\int_{(E^L(E'))}^{E^u(E')} P_3^i(E';\underline{r},E'')dE''} \tag{A.52}$$

$$= \frac{1}{E\sqrt{1-\frac{\epsilon}{E}}}\bigg/ U \quad , \quad \text{for } E^L(E') \le E \le E^u(E') \quad ,$$

where

$$U = \int_{E^L(E')}^{E^u(E')} \frac{1}{E''\sqrt{1-\epsilon/E''}} \, dE'' \tag{A.53}$$

$$= \ell n \left\{ \frac{[1+y(-1)]^2[1-y(1)^2]}{[1-y(-1)^2][1+|y(1)|]^2} \right\} \quad .$$

The density function h_3^i of Eq. (A.52) may be sampled analytically for E. The analytic expression is obtained by setting the cumulative distribution function to a random number F and solving for E:

$$F = \int_{E^L(E')}^{E} \frac{1}{E''\sqrt{1-\epsilon/E''}} \, dE'' \bigg/ U$$

$$= \ell n \left\{ \frac{\sqrt{E^2 - \epsilon E} + E - \epsilon/2}{\frac{\epsilon}{2}[1+|y(1)|]^2/[1-y(1)^2]} \right\} \bigg/ U \quad . \tag{A.54}$$

Hence, solving for E, we obtain

$$E = \beta^2/(2\beta - \epsilon) \quad , \qquad (A.55)$$

where

$$\beta = \frac{\epsilon}{2} \frac{[1 + |y(1)|]^2}{1 - y(1)^2} e^{\xi U} + \frac{\epsilon}{2} \quad . \qquad (A.56)$$

The pseudoneutron weight is obtained from Eqs. (24), (A.45), and (A.52) as

$$\overline{W} = \frac{\overline{W}' \Sigma_3^i(\underline{r},E)_\ell C_3^i(E', -\underline{\Omega}_a';\underline{r},E, -\underline{\Omega}_a)_\ell}{\Sigma_t(\underline{r},E')\overline{Q}_3(j,k,i,\ell)\overline{F}_3(E,\underline{\Omega}_a;\underline{r},E',\underline{\Omega}_a')} \qquad (A.57)$$

$$= \frac{\overline{W}' \Sigma_3^i(\underline{r},E)_\ell v_3^i(\underline{r},E)_\ell D_3^i(\mu_{cm};\underline{r},E)_{cm}(A + 1)^2 U}{\Sigma_t(\underline{r},E')\overline{Q}_3(j,k,i,\ell)2A} \quad ,$$

where the density function $D_3^i(\mu_{cm};\underline{r},E)_{cm}$ for the center-of-mass scattering angle has been inserted in Eq. (A.57) to include the more general case of anisotropic scattering. The pseudoneutron energy E is selected from the density function obtained with the isotropic scattering assumptions. However, this should not introduce large statistical errors unless the scattering is highly anisotropic.

The expression for U in Eq. (A.53) may be simplified as

$$U = \ell n \left(\frac{A + 1}{A - 1}\right)^2 \quad , \quad (A + 1)^2 E'/\epsilon > 1 \quad , \quad (A.58)$$

and

$$U = \ell n \left\{ \frac{1 + y(-1)}{1 - y(-1)} \frac{1 + y(1)}{1 - y(1)} \right\} \quad , \quad (A + 1)^2 E'/\epsilon < 1 \quad . \qquad (A.59)$$

4. Fission

The treatment of fission is simplified by the assumption that the energy spectrum of fission neutrons is independent of the energy of the parent neutron. The selection of a fission event with the probability $\overline{Q}_4$ (j,k,j') requires that the final pseudoneutron energy E be within the boundaries of energy group j', designated here as $(E^L)_{j'}$ and $(E^u)_{j'}$. The energy E within this group is selected from a uniform distribution as

$$E = (E^L)_{j'} + \left[(E^u)_{j'} - (E^L)_{j'}\right] \xi \quad , \qquad (A.60)$$

where ξ is a random number on the unit interval. The final pseudoneutron direction of motion is selected from an isotropic distribution in the laboratory system, and the weight is obtained from Eq. (24) as

$$\overline{W} = \frac{\overline{W}' \sum_i v_4^i(\underline{r},E)\Sigma_4^i(\underline{r},E)\gamma(E')\left[(E^u)_{j'} - (E^L)_{j'}\right]}{\Sigma_t(\underline{r},E')\overline{Q}_4(j,k,j')} \quad , \qquad (A.61)$$

where the subscript 4 denotes fission, $\gamma(E')$ is the spectrum of fission neutrons, and the fission neutrons are assumed to have an isotropic distribution in the laboratory system.

APPENDIX B

INPUT DATA FOR MCNA

The card format of the input data is identical to that of the MCN code except that there are no provisions for R(repeat) or I(interpolate) options. A brief description of the format of the input data follows.

Columns 1 to 5 are used to identify the input data on the card (a blank field in these columns indicates a continuation from the previous card, but a data entry may not be split between cards),

Data entries are contained in columns 6 to 72 with a comma or at least one blank column separating the entries,

A completely blank card in columns 1 through 72 designates the end of a block of data. Columns 73 to 80 are ignored and therefore may be used for sequencing.

The input data required for the initiation (Step 1 in Fig. 1) of MCNA are identical to those required for the initiation of the MCN code. A

description of the input data for the initiation is given in Refs. 4, 5, and 6. The following additional comments pertinent to MCNA may be useful.

1. An RO card should not be supplied if a thermal treatment isn't being used; i.e., EBR ≤ ECF.

2. The F, E, T, and C cards are not usually required in MCNA. An exception occurs during scoring in the adjoint sampling for a point neutron source; for this option see the description of the DFS input card in this appendix.

The input data pertinent to the coupled sampling in MCNA (Steps 2 and 4 of Fig. 1) will now be described. The usual procedure is to input all the required data for the coupled sampling in Step 2 so that additional input data are not required in Step 4 unless it seems advisable to change some data after the initial sampling from the transport equation. The ANUI program is called in Steps 2 and 4, and, in turn, reads the input data. The sequence of input card types is not important except that the first card must have the identifier TYP and the code expects to read this card each time the program ANUI is called. A blank card designates the end of input. The input data are as follows.

Card Identifier Columns (1-5)	Data Entry	Description of Data Columns (6-72)
TYP		Type of Calculation Card.
	1st	= -1, Initiation is completed, and preparation is now made to begin coupled sampling. After this input data, the coupled sampling will proceed to Step 3 of Fig. 1. Cards ASI, AE, and SCC must be input, and the rest of the data may be input as needed.
		= 0, Initiation is completed, but only sampling from the transport equation will be done. Steps 4 and 5 of Fig. 1 will be omitted. No more input allowed.
		= 1, Initiation is completed. Construct the adjoint sampling functions numerically and proceed directly to Step 5 of Fig. 1 (i.e., skip steps 3 and 4), sampling from the adjoint equation. Cards ASC, ASI, AF, AE, SCC, and FWE must be input, with other cards as required.
		= 2, Step 3, sampling from the transport equation, has been completed. Normalize* sampling functions and proceed to Step 5, sampling from the adjoint equation. No more input allowed.
		= 3, Same as = 2 except that changes in any of the cards ASC, ASP, ST, ASI, AF, ALE, and MN may be made.
		= 4, Sampling functions have already been normalized, but changes in any of the cards ASC, ASP, ST, ASI, AF, ALE, and MN may be made.
	2nd	= 0, Multigenerations are assumed.
		= 1, The calculation will be made for only one (pseudo) neutron generation. This effectively sets the number of neutrons per fission to zero.
	3rd	= Tape dump number. Usually this entry = 1 if the first entry on this card is -1, 0, or 1. This entry usually equals the last tape dump if the first entry is 2, 3, or 4. Exceptions sometimes occur when one tries sampling from the adjoint equation with slightly different input data from those used in a previous sampling.

*A sampling probability may be estimated as exactly zero after sampling from the transport equation. The code will check the corresponding transfer cross section, and if it is nonzero, the sampling probability will be normalized to a certain fraction of the total (usually about 1%).

Card Identifier	Data Entry	Description of Data
ASC		Adjoint Source Control Card
	1st	Energy Control

= 0, Select the initial pseudoneutron energy with a density function proportional to 1/E between the first and second data entries on card ASP.

= 1, Initial pseudoneutron energy set to 1st data entry on card ASP.

= 2, Linear selection of initial energy between the first and second data entries on card ASP.

= 3, Input an energy density table on card ST1.

≥ 4, Supply source routine ASOURC. The remainder of this card is not used in ANUI, except to specify tables ST1 to ST7.

2nd   Spatial Position Control

= 1, X = 3rd data entry on card ASP
Y = 5th data entry on card ASP
Z = 7th data entry on card ASP.

= 2, Linear selection from 3rd to 4th, 5th to 6th, 7th to 8th data entries on card ASP for X,Y,Z, respectively.

= 3, Input X,Y,Z density tables on cards ST2, ST3, ST4, respectively.

= 0, Constant-volume source in the cell specified by the 5th data entry of this card. Only the volume between concentric spheres presently available.

3rd   Direction-of-Motion Control

= 1, $v = \cos$ (9th data entry on card ASP)

$w = \sqrt{1 - v^2} \cos$ (10th data entry on card ASP)

$u = \sqrt{1 - v^2} \sin$ (10th data entry on card ASP).

= 2, Isotropic distribution.

= 3, Input density tables on cards ST5 and ST6.

4th   Time Control

= 1, TME = 11th data entry on card ASP.

= 2, LINEAR selection of TME from 11th to 12th data entries on card ASP.

= 3, Input time density table on card ST7.

5th   = Cell number of pseudoneutron source, IA.

6th   = 0, Ignore.

= 1, Call subroutine ASOURC after "built-in" routines are used to select initial pseudoneutron parameters (see example problem of Sec. IV for an application of this option).

ASP   Adjoint Source Parameter Card

1st to 12th   Entries as specified on card ASC. Those not specified on card ASC will not be used in sampling, but must be input as zeros.

Card Identifier	Data Entry	Description of Data
ST1		Adjoint Source Energy Table (Required if the first data entry of card ASC = 3).
	1st to Nth	N/2 energy values from low to high and the corresponding N/2 cumulative probabilities (the first probability is zero and the last is one). NOTE: If this table is used with the first data entry on card ASC set to 3, then the initial pseudoneutron weight is divided by this density function. This is not true for tables ST2 to ST7.
ST2		Adjoint Source X Table (Required if the second data entry of card ASC = 3).
	1st to Nth	Not necessarily the same N as for card ST1. N/2 X values from low to high and the corresponding N/2 cumulative probabilities.
ST3		Adjoint Source Y Table
	1st to Nth	Same as card ST2 for Y.
ST4		Ajoint Source Z Table
	1st to Nth	Same as card ST2 for Z.
ST5		Adjoint Source Direction Table (Required if the third data entry of card ASC = 3). $v = \cos$ (selection from this table).
	1st to Nth	N/2 values and corresponding N/2 cumulative probabilities.
ST6		Adjoint Source Direction Table (Required if the third data entry of card ASC = 3). $w = \sqrt{1 - v^2} \cos$ (selection from this table) $u = \sqrt{1 - v^2} \sin$ (selection from this table)
	1st to Nth	N/2 values and corresponding N/2 cumulative probabilities.
ST7		Adjoint Source Time Table (Required if the fourth data entry of card ASC = 3).
	1st to Nth	N/2 time values from low to high and corresponding N/2 cumulative probabilities.

NOTE on cards ST1 to ST7. Any or all of these tables may be used and the tables may have different lengths, but the total storage required (sum of the N's) must be less than 401.

Card Identifier	Data Entry	Description of Data
ASI		Adjoint Sampling Information Card
	1st	= -1, Select the pseudoneutron energy after inelastic scattering from a density function, Eq. (A.36), proportional to the transfer cross section each time the energy, E, is less than 2 MeV. For energies greater than 2 MeV, use constant-density functions, Eq. (A.21).
		= 0, Same as -1 except that for energies greater than 2 MeV, select the energy E from within the energy band using a density function proportional to the fission spectrum for both fission and inelastic scattering. This is a useful option if the neutron source is a fission spectrum.

ASI		= 1, Assume constant-density functions in intervals.
		Comment: -1 suggested for most applications.
	2nd	= 0, Initial pseudoneutron weight set to the fourth data entry on this card.[*]
		= 1,2,3,4, The initial pseudoneutron weight is set to the fourth data field on this card multiplied by $\Sigma_f(\underline{r},E), \nu\Sigma_f(\underline{r},E), \Sigma_c(\underline{r},E),$ or $\Sigma_t(\underline{r},E)$, respectively.[*]
	3rd	= 0, Hydrogen transfer tables will not be constructed; $\beta(j,k,\gamma)$ of Eq. (A.11).
		= Energy group number (see card AE) to start hydrogen transfer tables. For groups less than this number, the center-of-mass scattering angle is selected isotropically. This number must always be less than the total number of groups and must be greater than 10 when a thermal-energy treatment is used.
	4th	Initial pseudoneutron weight as defined by the 2nd data entry on this card.
	5th	Terminate the pseudoneutron with this probability at each collision when the energy is greater than 6 MeV. The surviving pseudoneutrons have their weight divided by one minus this probability. Zero suggested for most applications.
	6th	A positive floating-point number will force the pseudoneutron weight to be split each time the weight exceeds this entry. A negative floating-point number will force splitting or "Russian roulette" to keep the weight at exactly the negative of this entry. For most applications it is recommended that this number be positive, and of such a magnitude that only occasionally will a pseudoneutron weight exceed it.
	7th	The total number of fission neutrons produced in the transport sampling will be divided by this number to construct the functions for sampling from the adjoint equation. Usually set to 1.0.
AF_ $\underline{N}$		Functional Card for Function N, N ≤ 350.
	0th to ≤ 8th	Constants to describe this functional (≤ 8). These constants are set to (AJCON(N,J), J = 1, K) for use in scoring in subroutine SCORE. Here, K is the number of constants entered on this card. The present dimensions allow as many as 350 functionals, but only a maximum of 50 sets of constants may be input. Cards for all the functionals need not be input, but the card for maximum N must be input.
ALE		Adjoint Leakage Card.
	1st	= 0, Special leakage computations are not utilized (in which case this card is not required).
		> 0, Computes leakage probability ANL = $e^{-\int_0^{X_s} \Sigma_t(\chi)dx}$ after each collision when the pseudoneutron energy is such that ESURL < E < ESURH and calls subroutine SCORE with KASR = 4. Here χ_s is the distance to a surface(s) of interest. ESURL and ESURH are the 2nd and 3rd data entries on this card, respectively. If E is not within these bounds, the usual distance-to-collision geometry routine is used.

---

[*]If subroutine ASOURC is supplied, the weight must be set in ASOURC. If Table T1 is used, the weight given by the second data entry on card ASI is also divided by the energy-density function as computed for each source pseudoneutron. If the first data entry on card ASC is zero, the weight given by the second data entry on card ASI is also divided by the energy-density function as computed for each source pseudoneutron; i.e., weight multiplier is $E \ln(E_{max}/E_{min})$.

Card Identifier	Data Entry	Description of Data
ALE		= 1, For ESURL < E < ESURH, sample the distance to collision from the exponential density function normalized so that leakage does not occur.
		= 2, Sample the distance to collision from the usual exponential density function, Eq. (16), using the special leakage routine when ESURL < E < ESURH. This is faster than returning to the geometry routine, when ANL must be computed anyway.
		= 3, Special optimal distance-to-collision sampling, Eq. (C.5)[*].
		= 4, Return to geometry routine for distance-to collision sampling after computing ANL
	2nd	As defined on the first data entry of this card.
	3rd	As defined on the first data entry of this card.
	4th to ≤ 23rd	Scoring surface numbers, JA. ANL is computed, and subroutine SCORE is called each time the projected pseudoneutron flight path, with ESURL < E < ESURH, crosses one of these surfaces. The pseudoneutron is expected to cross one, and only one, scoring surface if the first entry on this card is 1, 2, or 3.
MN _ N		Thermal Flux Weight Card (required only if the thermal free-gas model is used).
	1st	= 0, Maxwellian weight factor for thermal group 1 and time increment N; i.e., $\Phi(E)$ of Eq. (A.14) equals $Ee^{-E/T}$. If N = 1, this weight factor is used for times less than the first data entry on the RO card of the initiation input data. If N = 2, this weight factor is used for times between the first and second data fields of the RO card, and so forth.
		= 1, Weight factor of 1/E for thermal group 1 and time increment N.
	2nd to 10th	Same as the first data entry description for subsequent thermal energy groups, low to high energies.
		NOTE: A weight factor of 1/E is not presently allowed for the first group if hydrogen is present, or for the first three groups if deuterium is present.
AEO		Energy Group Boundaries Card
	1st	> 0, Equal to the total number, ≤ 50, of energy groups (for constructing the functions for sampling from the adjoint equation) that are read on card AE_N. If a thermal treatment is used, the first ten groups must be thermal.
		≤ 0, A routine in the code will construct the energy group boundaries.
		= -2, For energies greater than 20 keV, construct one-quarter lethargy energy group widths and one-quarter lethargy energy increments for the inelastic scattering with a continuous model.
		= -1, Same as -2 control except that the inelastic increments are one-half lethargy.

---

[*]The volume of each cell VOL(IA) must be supplied in Program ANUI in order to use this option.

Card Identifier	Data Entry	Description of Data
AE0		= 0, For energies greater than 20 keV, construct one-half lethargy energy group widths and one-half lethargy energy increments for the inelastic scattering with a continuous model. This option has been found adequate for most problems. NOTE: If this data entry ≤ 0, the energy group widths from thermal to 1 keV are constructed at one lethargy unit, and from 1 to 20 keV at one-half lethargy unit. Only four inelastic increments are used in this range.
	2nd	Maximum energy for constructing the energy-group structure (generally the maximum energy of interest in the problem).
	3rd to 12th	These data entries are required only when a thermal treatment is utilized and the first data field on this card is ≤ 0. These entries are the top boundaries of the 10 thermal groups, from low to high (group number 10 must be EBR). These energy groups are used in cells where hydrogen or deuterium are not present. In regions where hydrogen or deuterium are present, the upper boundaries are set by the code as: 0.1T, 0.5T, T, 1.5T, 2.5T, 4T, 6T, 6T + (EBR-6T)/7, 6T + 3(EBR-6T)/7, and EBR, where T is the temperature of the medium at the time of interest and EBR is the upper boundary of the thermal treatment.
AE N		Energy Group Boundaries Card (required only if the first data entry on card AE0 > 0). These AE N cards must be input in sequential order with N assuming integer values from 1 to the number of energy groups specified by the first data field on card AE0. The energies (first data entries) are input monotonically increasing from low to high values.
	1st	Upper energy boundary of group N. For a thermal treatment with N ≤ 10, these are thermal boundaries, and for N = 10 this data entry must be set to EBR.
	2nd to 51st	Widths of the energy increments (low to high) for inelastic scattering of the pseudoneutron with a continuous model for energy group N, i. e., the ΔE_β, of Eq. (A.21). The sum of these increments plus the upper boundary of group N-1 should be greater than or equal to the second data entry on card AE0. This is checked by the code.
SCC		Sampling Cell Control Card
	1st	Control parameter for cell No. 1; IA = 1. It controls the construction and use of the density function for sampling from the adjoint equation. = -1, Cell is a vacuum. = 0, Construct sampling functions for this cell. = I, Lump this cell with cell I for the construction and use of sampling functions, I < IA. This option is available only if the same isotopes are in both cells and is useful if one cell is very small because the statistical fluctuations in the density functions are reduced with this option.
	2nd to the number of cells	Same as the first data entry for subsequent cells.
DFS		Delta Function Scoring Card
	1st	= 0, Special neutron point source option for scoring in the adjoint calculation is not utilized (in which case this card is not required).

Card Identifier	Data Entry	Description of Data
DFS		= 1, Special neutron point source option for scoring in the ad- joint calculation is utilized (see Appendix E for a discus- sion of the scoring). The F5 card in the initiation (with program AITMC) is utilized to specify the X, Y, Z, and neighborhood of the point sources. Only one energy entry and one time entry, respectively, are required on the E5 and T5 cards. These entries are ignored in the adjoint sampling but are required for memory allocation.
	2nd	Minimum energy of the point sources, i.e., energy below which no neutrons are emitted. This energy must be greater than the thermal cutoff energy, EBR.
	3rd	Maximum energy of the point sources.
		NOTE: The ALE card, with the first entry equal to 1, may be used with this point source scoring option.
IO		Cell Importance Card (may be used to change cell importances from those specified in the initiation).
	1st to the number of cells	Importance of the respective cells.

The following two cards are used only if the first data entry on card TYP is 1.

FWE		Flux Weight Card
	1	Control parameter for cell No. 1, IA = 1. This parameter con- trols the numerical computation of the density functions for sampling from the adjoint equation. The analog density function is multiplied by an estimate of the average energy dependence of the neutron flux in this cell.

= 0, Constant flux as a function of energy.

= -1, The neutron flux φ is given by

$$\varphi = E^{1/2} \, e^{-0.776E} \text{ for } E > 1,$$

$$\varphi = \left(0.7315 + 0.1174 \, \ell n \frac{E}{10}\right) \Big/ E \text{ for } 0.04 < E < 1,$$

$$\varphi = 0.08328/E \text{ for } E < 0.04.$$

= -2, $\varphi = \sqrt{E} \, e^{-0.776E}$

= -3, $\varphi = \sqrt{E} \, e^{-0.776E}$ for $E > 0.1$

$\qquad \varphi = 0.029262/E$ for $E < 0.1$

= -4, $\varphi = \sqrt{E} \, e^{-0.776E}$ for $E > 0.1$,

$\qquad \varphi = 0.29262$ for $E < 0.1$

= -5, $\varphi = 1/E$

= -6, $\varphi = \sqrt{E} \, e^{-0.776E}$ for $E > 0.6443$

$\qquad \varphi = 0.3136/E$ for $E < 0.6443$

= -7, $\varphi = \sqrt{E} \, e^{-0.776E}$ for $E > 0.6443$

$\qquad \varphi = 0.4868$ for $E < 0.6443$

= -8, $\varphi = 1/V$

= N, A table of length N, N > 0, is input on card FTB_1 for a
tabulation of the neutron flux.

Card Identifier	Data Entry	Description of Data
FWE	2nd to the number of cells	Same as the first data entry for subsequent cells.
FTB_I		Flux Value Card
	1 to N	N/2 energy points followed by N/2 flux values for cell I. The energy points are from low to high, and the code linearly interpolates between energy points.
Blank Card		END OF INPUT DATA

A few additional comments may prove worthwhile.

1. The maximum dimensions of input quantities are given for the present code. These are usually simple to change, and the code checks the dimension quantities to see that storage is not exceeded. The memory required by the sampling functions is checked after loading, and the problem is terminated with an error message if any dimensions are exceeded. This is checked prior to sampling from the transport equation.

2. Blank columns are ignored when reading the card identifier in columns 1 to 5. Thus, the card AF_N with N = 3 could appear as

$$
\begin{array}{l}
\text{AF3} \\
\text{AF } 3 \\
\text{AF 3} \\
\text{AF3} \\
\text{AF 3} \\
\end{array}
$$
etc.

The units used in the MCNA code and in the input data are consistent with those of the MCN code; i.e., energies are in MeV, time is in shakes, macroscopic cross sections are in cm^{-1}, medium temperatures are in MeV, and spatial dimensions are in cm. The units of the functionals may be controlled by the functional constants of card AF and the initial pseudoneutron weight of card ASI.

The use of the pseudoneutron source subroutine, ASOURC, with the first data entry of card ASC ≥ 4, automatically bypasses all the built-in adjoint source options on cards ASC and ASP. The following information must be supplied (an exception occurs when the sixth data entry of card ASC = 1 and the first data entry of card ASC < 4) when ASOURC is used.

x,y,z - the space coordinates

u,v,w - the direction coordinates, these are isotropic if not supplied

TME - the time

ERG - the energy

WT - the initial weight. The initial weight as input on the fourth data entry of card ASI is the parameter ASRWT, and WT = ASRWT at entrance to ASOURC. Options 1, 2, 3, 4 of the second data entry of card ASI are not available when using ASOURC unless the sixth data entry of card ASC = 1.

IA - the cell number

JA - surface control (usually 1)

DEL - surface control (usually 0.0).

Special care should be used in writing subroutine SCORE, to tabulate the functionals. The functional K is tabulated in the dimension variable TSCOR(K). The general procedure each time SCORE is called is as follows.

1. Check to see if the collision or surface crossing is of interest; determined by KASR as described in Sec. III. If not of interest, return to the main program.

2. Check to see if the collision or surface crossing is of interest for functional K. If so, score as

$$TSCOR(K) = TSCOR(K)$$

$$+ \begin{bmatrix} \text{contribution of this collision or surface} \\ \text{crossing to the functional K.} \end{bmatrix}$$

(B.1)

3. Repeat step 2 for all functionals and return to the main program. See Sec. III for two examples.

The scoring in Eq. (B.1) may require some constants for the particular functional K. These constants may be input on the AF card in the dimensioned variable AJCON(K,J), where J assumes values from 1 to the number of required constants for the

functional K.

At the end of each source (and progeny) pseudoneutron history, TSCOR(K) and the 2nd, 3rd, and 4th moments of TSCOR(K) are added to a running sum of the respective first four moments for each functional K. TSCOR(K) is then set to zero before selecting the next source pseudoneutron. Periodically during the sampling from the adjoint equation, these moments are divided by the total number of source pseudoneutrons to obtain the estimate of the functional $\overline{T_K}$ and the estimate of the moments $\overline{T_K^2}$, $\overline{T_k^3}$ and $\overline{T_K^4}$. The estimated relative error is computed as

$$\text{Relative error} = \sqrt{\overline{T_K^2} - \overline{T_K}^2} \Bigg/ \left[\overline{T_K} \sqrt{n} \right] \qquad (B.2)$$

where n is the total number of source pseudoneutrons. Unfortunately, there is also a statistical error involved in the estimate of the relative error. An attempt is made in MCNA to estimate this as[17]

$$\sqrt{\overline{T_k^4} - 4\overline{T_K^3}\,\overline{T_K} + 6\overline{T_K^2}\,\overline{T_K}^2 - 4\overline{T_K}^4 - \overline{T_K^2}^2} \Bigg/ \sqrt{n} \left\{ \overline{T_K^2} - \overline{T_K}^2 \right\}^{3/2} .$$

$$(B.3)$$

Experience will tell whether Eq. (B.3) is of any help in determining the reliability of the relative error estimate of Eq. (B.2).

Two magnetic tapes are usually required to run a problem with MCNA. A description of the use of these tapes is given in the example problem in Sec. IV.

The program ATMC that samples from the transport or adjoint equations requires one input card, as in the MCN code. The input on this card is as follows.

Columns	Transport Sampling (Step 3)	Adjoint Sampling (Step 5)
1-10	Neutrons are terminated at this entry of maximum time.	Pseudoneutrons are terminated at this entry of minimum time.
11-20	Neutrons are terminated when their weights fall below this entry.	"Russian roulette" is played each time a pseudoneutron weight falls below this entry. The weights of survivors are increased.
21-30	Running time in minutes.	Running time in minutes.
31-40	Number of neutron histories per print cycle.	Number of pseudoneutron histories per print cycle.
41-50	Number of neutron histories per tape dump cycle.	Number of pseudoneutron histories per tape dump cycle.
51-60	Tape dump number (usually 2 for the first time in Step 3 of Fig. 1).	Tape dump number.
61-70	Total number of neutron histories.	Total number of pseudoneutron histories.

APPENDIX C

DISTANCE-TO-COLLISION DISCUSSION

Use of the exponential density function $T(\chi)$ of Eq. (16) has the practical advantage that the distance to collision χ may be sampled from a simple analytic expression. The fact that it also simulates the physical process, when sampling from the transport equation, adds to its versatility in numerous applications.

The use of $T(\chi)$ for sampling the distance to collision of pseudoneutrons has also been found adequate in many adjoint problems. However, the use of $T(\chi)$ is not so satisfactory in some cases. This is apparently because $T(\chi)$ is a poor approxi-

mation to the corresponding zero-variance density function in these problems.

The zero-variance density function $T_o(\chi)$ is given by

$$T_o(\chi) = \frac{T(\chi)\beta(\chi)/\Sigma_t(\chi)}{\int_0^\infty T(\chi')\beta(\chi')/\Sigma_t(\chi')d\chi'} \quad , \qquad (C.1)$$

where $\beta(\chi)$ is an appropriate limit of the rate at which neutrons (in the transport problem) suffer collisions and emerge from the collisions with the energy of the pseudoneutron and with their direction of flight opposite to that of the pseudoneutrons. The function $\beta(\chi)$ generally depends upon the direction of motion of the pseudoneutron, its energy, and the spatial position χ. Here the energy and direction of motion are suppressed in the arguments of $\beta(\chi)$ owing to notation difficulties. It is understood that β is evaluated along the projected flight path of the pseudoneutron and at the pseudoneutron energy.

The directional dependence of $\beta(\chi)$ is often nearly isotropic within most of the phase space, and, for the applications in MCNA, it is assumed to be isotropic. It is also assumed that, within a cell and an energy group, $\beta(\chi)$ is approximately constant. With these assumptions, $\beta(\chi)$ may be approximated by its average value within a cell k and energy group j as

$$\beta_{jk} = \frac{\iint_{cell_k} \int \iint_{(E_L)_j}^{(E_u)_j} \varphi(\underline{r},E,\underline{\Omega}) \Sigma_t(\underline{R},E)C(E',\underline{\Omega}';\underline{r},E,\underline{\Omega}) \, dE' \, d\underline{\Omega}' \, d^3r dE d\underline{\Omega}}{\int_{cell_k} \int_{(E_L)_j}^{(E_u)_j} dE' d^3r} \quad . \qquad (C.2)$$

An option is available in MCNA to compute the quantities β_{jk} by sampling from the transport equation. These average values for $\beta(\chi)$ are subsequently used in Eq. (C.1) to obtain an approximation to the zero-variance density function as

$\overline{T}(\chi)_{\chi \text{ in cell } k}$

$$= e^{-\sum_{k'=1}^{k-1} \Sigma_{tjk'}\Delta\chi_{k'}} e^{-\Sigma_{tjk}\left(\chi - \sum_{k'=1}^{k-1}\Delta\chi_{k'}\right)} \beta_{jk}\bigg/ H \, , \quad (C.3)$$

where

$$H = \sum_{m=1}^{N} e^{-\sum_{m'=1}^{m-1} \Sigma_{tjm'}\Delta\chi_{m}'} \left(1 - e^{-\Sigma_{tjm}\Delta\chi_m}\right)\beta_{jm}\bigg/\Sigma_{tjm} \quad . \tag{C.4}$$

Here, the notation has been simplified by numbering the subsequent cells of the flight path of the pseudoneutron by $k = 1, 2, 3 \cdots N$. The corresponding total cross sections are denoted by Σ_{tjk} (this is poor notation because it really denotes the total cross section at the energy of the pseudoneutron), and the distances across the cells by $\Delta\chi_k$. The distance to collision χ may be sampled with the density function $\overline{T}(\chi)$ of Eq. (C.3) as

$$\chi = \sum_{k'=1}^{k-1} \Delta\chi_{k'}$$

$$-\frac{1}{\Sigma_{tjk}} \ln\left\{1 + \frac{\Sigma_{tjk}}{y_{k-1}\beta_{jk}}\left[\left(\sum_{m'=1}^{k-1}(y_{m'-1} - y_{m'})\frac{\beta_{jm'}}{\Sigma_{tjm'}}\right) - \xi H\right]\right\} , \tag{C.5}$$

where ξ is a random number on the unit interval, y_m' is computed as

$$y_{m'} = e^{-\sum_{m''=1}^{m'} \Sigma_{tjm''} \Delta\chi_{m''}} \quad , \quad m' > 0 \quad , \qquad (C.6)$$

$$y_o = 1 \quad ,$$

and the cell k is determined by finding the cell that satisfies the requirement

$$\frac{1}{H}\sum_{m=1}^{k-1}(y_{m-1} - y_m)\frac{\beta_{jm}}{\Sigma_{tjm}} < \xi \leq \frac{1}{H}\sum_{m'=1}^{k}(y_{m'-1} - y_{m'})\frac{\beta_{jm'}}{\Sigma_{tjm'}} \quad . \tag{C.7}$$

The pseudoneutron weight is then obtained as

$$\overline{W} = \overline{W'} \; T(\chi) / \overline{T}(\chi) \quad ,$$

$$= \overline{W'} \; \Sigma_{tjk} H / \beta_{jk} \quad . \qquad (C.8)$$

The indications (from the problems that have been solved using this procedure to sample for the distance to collision) are that the variance per source pseudoneutron is reduced from the variance obtained by sampling from the adjoint equation with the analog density function $T(\chi)$. However, the sampling time per source pseudoneutron may increase by as much as a factor of two or even more. It is fortunate that the analog density function $T(\chi)$ is satisfactory for most applications. For problems for which it is not satisfactory, the density function $\overline{T}(\chi)$ of Eq. (C.3) may help, but the added sampling time required to sample from $\overline{T}$ reduces its effectiveness. However, the option is available in the MCNA code.

APPENDIX D

MISCELLANEOUS PROBABILITY CONCEPTS

1. Linear Interpolation of Density Functions

A density function $g(\chi';\chi)$ is sometimes tabulated in MCN and MCNA at the points χ_1 and χ_2 with $\chi_1 < \chi < \chi_2$. The sampling of the neutron history requires that the random variable χ' be selected from $g(\chi';\chi)$. This is accomplished with a random variable ξ on the unit interval and linear interpolation as

$$\chi' = \chi'_1 + (\chi - \chi_1)(\chi'_2 - \chi'_1)/(\chi_2 - \chi_1) \quad , \quad (D.1)$$

where χ'_1 and χ'_2 satisfy the inverse relations

$$\xi = \int_{-\infty}^{\chi'_1} g(\chi'';\chi_1) d\chi'' \quad , \qquad (D.2)$$

$$\xi = \int_{-\infty}^{\chi'_2} g(\chi'';\chi_2) d\chi'' \quad . \qquad (D.3)$$

The sampling of the pseudoneutron history requires computation of the actual density function $g(\chi';\chi)$ to compute the weight of the pseudoneutron. If $G(\chi';\chi)$ is defined to be the cumulative distribution function, then, from Eqs. (D.2) and (D.3), it must satisfy

$$G(\chi';\chi) = G(\chi'_1;\chi_1) = G(\chi'_2;\chi_2) \quad , \qquad (D.4)$$

where χ', χ'_1 and χ'_2 are related by Eq. (D.1). The distribution function $g(\chi';\chi)$ may be expressed as

$$g(\chi';\chi) = \frac{dG(\chi';\chi)}{d\chi'} = \frac{dG(\chi'_1;\chi_1)}{d\chi'_1} \frac{d\chi'_1}{d\chi'} \quad . \qquad (D.5)$$

The derivatives may be obtained from Eq. (D.1), (D.2), and (D.3) as

$$\frac{dG(\chi'_1;\chi_1)}{d\chi_1} = \frac{d}{d\chi'_1} \int_{-\infty}^{\chi'_1} g(\chi'';\chi_1) d\chi'' = g(\chi'_1;\chi_1) \qquad (D.6)$$

$$\frac{d\chi'}{d\chi'_1} = \frac{\partial \chi'}{\partial \chi'_1} + \frac{\partial \chi'}{\partial \chi'_2} \frac{d\chi'_2}{d\chi'_1}$$

$$= 1 - \frac{(\chi - \chi_1)}{(\chi_2 - \chi_1)} + \frac{(\chi - \chi_1)}{(\chi_2 - \chi_1)} \frac{g(\chi'_1;\chi_1)}{g(\chi'_2;\chi_2)} \quad , \qquad (D.7)$$

where $d\chi'_2/d\chi'_1$ was obtained by combining Eqs. (D.2) and (D.3). With Eqs. (D.6) and (D.7), the density function of Eq. (D.5) may be expressed as

$$g(\chi';\chi) = \frac{g(\chi'_1;\chi_1)}{1 - \frac{(\chi - \chi_1)}{(\chi_2 - \chi_1)} + \frac{(\chi - \chi_1)}{(\chi_2 - \chi_1)} \frac{g(\chi'_1;\chi_1)}{g(\chi'_2;\chi_2)}}$$

$$= \frac{g(\chi'_1;\chi_1) g(\chi'_2;\chi_2)}{\left[1 - \left(\frac{\chi - \chi_1}{\chi_2 - \chi_1}\right)\right] g(\chi'_2;\chi_2) + \frac{(\chi - \chi_1)}{(\chi_2 - \chi_1)} g(\chi'_1;\chi_1)} \quad .$$

$$\qquad (D.8)$$

2. Sampling the Weighted Free-Gas Density Function

The density function b_1^i of Eq. (A.14) may be expressed as the product of a marginal density function g_1^i for selecting the energy E and a conditional density function h_1^i for selecting the laboratory scattering angle μ_L. These density functions are determined in the usual manner as

$$g_1^i(E;\underline{r},E') = \int b_1^i(E,\underline{\Omega}_a;\underline{r},E',\underline{\Omega}_a')d\underline{\Omega}_a$$

$$= \frac{\Sigma_1^i(\underline{r},E)c_1^i(E';\underline{r},E)\Phi(E)_{j'}}{\int_{(E_L)_{j'}}^{(E_u)_{j'}} \Sigma_1^i(\underline{r},E'')c_1^i(E';\underline{r},E'')\Phi(E'')_{j'}\,dE''},$$

(D.9)

$$h_1^i(\mu_L;\underline{r},E',E) = \frac{2\pi b_1^i(E,\underline{\Omega}_a;\underline{r},E',\underline{\Omega}_a')}{g_1^i(E;\underline{r},E')}$$

$$= \frac{2\pi c_1^i(E',-\underline{\Omega}_a';\underline{r},E,-\underline{\Omega}_a)}{c_1^i(E';\underline{r},E)},$$

(D.10)

where $c_1^i(E';\underline{r},E)$ is defined as

$$c_1^i(E';\underline{r},E) = \int c_1^i(E',-\underline{\Omega}_a';\underline{r},E,-\underline{\Omega}_a)d\underline{\Omega}_a.$$

(D.11)

The density function g_1^i of Eq. (D.9) may be obtained by replacing $\Sigma_1^i(\underline{r},E)\,c_1^i(E';\underline{r},E)$ with the free-gas kernel as given, for example, by Eq. (2.19a) of Williams:[14]

$$g_1^i(E;\underline{r},E') = \frac{1}{E}\,\Phi(E)_{j'}\left\{e^{-(\epsilon'-\epsilon)}\left[\text{Erf}(\theta\sqrt{\epsilon}-\zeta\sqrt{\epsilon'})\right.\right.$$

$$\pm \text{Erf}(\theta\sqrt{\epsilon}+\zeta\sqrt{\epsilon'}) + \text{Erf}(\theta\sqrt{\epsilon'}-\zeta\sqrt{\epsilon})$$

$$\left.\left.\mp \text{Erf}(\theta\sqrt{\epsilon'}+\zeta\sqrt{\epsilon})\right]\right\}\bigg/U,$$

(D.12)

where U is the integral of the numerator of the right-hand side of Eq. (D.12) from $(E_L)_{j'}$ to $(E_u)_{j'}$, the $\mp$ signs are used for $E < E'$ or $E > E'$, respectively, and

$$\epsilon' = E'/T$$

(D.13)

$$\epsilon = E/T$$

(D.14)

$$\theta = (A + 1)/2\sqrt{A}$$

(D.15)

$$\zeta = (A - 1)/2\sqrt{A}.$$

(D.16)

An analytic expression for the corresponding cumulative distribution function G_1^i may be obtained when $\Phi(E)_{j'} = Ee^{-E/T}$, but G_1^i must be tabulated for $\Phi(E)_{j'} = 1/E$. In either case, it is impossible to obtain an expression for the inverse E in terms of G_1^i. The technique used in the MCNA code is to divide the range from $(E_L)_{j'}$ to $(E_u)_{j'}$ of E into equal segments, evaluate G_1^i at the segment boundaries, and linearly interpolate for E.

The analytic expression for G_1^i with $\Phi(E)_{j'} = Ee^{-E/T}$ is given by

$$G_1^i(E;\underline{r},E')$$

$$= \frac{T}{U}e^{-\epsilon}\left[\frac{4A}{(A+1)^2}\left[\theta^2\epsilon' - \zeta^2\epsilon - \frac{(A^2+2A-1)}{4A}T\right]\right.$$

$$[\text{Erf}(\theta\sqrt{\epsilon'}-\zeta\sqrt{\epsilon})\pm\text{Erf}(\theta\sqrt{\epsilon'}+\zeta\sqrt{\epsilon})]$$

$$+\frac{4A}{(A+1)^2\sqrt{\pi}}\left[(\theta\sqrt{\epsilon'}+\zeta\sqrt{\epsilon})e^{-(\theta\sqrt{\epsilon'}-\zeta\sqrt{\epsilon})^2}\right.$$

$$\left.\pm(\theta\sqrt{\epsilon'}-\zeta\sqrt{\epsilon})e^{-(\theta\sqrt{\epsilon'}+\zeta\sqrt{\epsilon})^2}\right]$$

$$+e^{(\epsilon-\epsilon')}[\text{Erf}(\zeta\sqrt{\epsilon'}-\theta\sqrt{\epsilon})$$

$$\left.\pm\text{Erf}(\zeta\sqrt{\epsilon'}+\theta\sqrt{\epsilon})]\right]_{(E_L)_{j'}}^{(E_u)_{j'}},$$

(D.17)

where the expression in Eq. (D.17) must be evaluated at the limits $(E_u)_j$ and $(E_L)_{j'}$. For in-group scattering (i.e., E and E' both in group j'), the expression must also be evaluated at the inner limit E', owing to the sign changes.

The density function h_1^i of Eq. (D.10) is the ratio of the free-gas scattering kernel for the energy and scattering angle, as given by Eq. (2.19) of Williams,[14] to the free-gas scattering kernel for the energy alone as given by Williams' Eq. (2.19a). The algebra involved in substituting these definitions into h_1^i and evaluating the cumulative distribution function H_1^i is tedious and will not be given

here. The result is that

$$H_1^i(\mu_L;\underline{r},E',E) = \left\{ \text{Erf}\left(\beta - \frac{\gamma}{\beta}\right) - \text{Erf}\left(\eta - \frac{\gamma}{\eta}\right)\right.$$

$$+ e^{4\gamma} \left. \text{Erf}\left[\left(\beta + \frac{\gamma}{\beta}\right) - \text{Erf}\left(\eta - \frac{\gamma}{\eta}\right)\right]\right\} \Bigg/$$

$$\left\{ \text{Erf}\left(\beta - \frac{\gamma}{\beta}\right) - \text{Erf}\left(\eta_1 - \frac{\gamma}{\eta_1}\right)\right.$$

$$+ e^{4\gamma} \left. \text{Erf}\left[\left(\beta + \frac{\gamma}{\beta}\right) - \text{Erf}\left(\eta_1 - \frac{\gamma}{\eta_1}\right)\right]\right\} \quad , \quad (\text{D.18})$$

where

$$\beta = \frac{1}{2\sqrt{AT}} \left(\sqrt{E} + \sqrt{E'}\right) \quad , \qquad (\text{D.19})$$

$$\eta = \frac{1}{2\sqrt{AT}} \left(E + E' - 2\mu_L\sqrt{EE'}\right)^{1/2} \quad , \qquad (\text{D.20})$$

$$\eta_1 = \frac{1}{2\sqrt{AT}} \left(E + E' - 2\sqrt{EE'}\right)^{1/2} = \frac{1}{2\sqrt{AT}} \left|\sqrt{E} - \sqrt{E'}\right| \quad ,$$

$$\gamma = (E - E')/4T \quad , \qquad (\text{D.21})$$

$$\text{Erf}(y) = \frac{2}{\sqrt{\pi}} \int_0^y e^{-u^2} du \quad . \qquad (\text{D.22})$$

It is impossible to obtain an inverse solution of Eq. (D.18) for μ_L. The technique utilized in the MCNA code is to divide the range from -1 to +1 of μ_L into equal segments, evaluate H_1^i at the segment boundaries, and linearly interpolate for μ_L.

APPENDIX E

SCORING IN THE ADJOINT CALCULATION

FOR A POINT NEUTRON SOUCE

1. Derivation of Scoring Equations at a Pseudoneutron Collision

The neutron souce is assumed to be of the form

$$S(\underline{r},E,\underline{\Omega},t) = S_\theta(E,\underline{\Omega},t)\delta(x - x_\theta)\delta(y - y_\theta)\delta(z - z_\theta) \quad ,$$

$$(\text{E.1})$$

where $S_\theta(E,\underline{\Omega},t)$ does not contain a delta function. A possible scoring technique in the adjoint calculation is to compute the density of neutrons emerging from their first collision and use this as the neutron source. At each pseudoneutron collision, the score is

$$\frac{\bar{W}*(\text{first-collision neutron source at } r',E',-\Omega',t')}{\Sigma_t(\underline{r}',E')} \quad ,$$

$$(\text{E.2})$$

where the pseudoneutron collision occurs at $\underline{r}',E',\underline{\Omega}',t'$.

A more practical procedure is to select the event α prior to the scoring with probability $\bar{Q}_\alpha(j,k,\cdots)$. Then the score is given by

$$\frac{\bar{W}*\left(\begin{array}{c}\text{first-collision neutron source at } \underline{r}',E',\underline{\Omega}',t' \\ \text{due to event of type } \alpha\end{array}\right)}{\Sigma_t(\underline{r}'E') \, \bar{Q}_\alpha(j,k,\cdots)} \quad .$$

$$(\text{E.3})$$

This gives the correct expectation; the expectation value of the score at the collision is given by

$$\frac{\sum_\alpha \bar{W}*\left(\begin{array}{c}\text{first-collision neutron source at} \\ \underline{r}',E',\underline{\Omega}',t' \text{ due to event of type } \alpha\end{array}\right) \bar{Q}_\alpha(j,k,\cdots)}{\Sigma_t(\underline{r}',E') \, \bar{Q}_\alpha(j,k,\cdots)}$$

$$= \frac{\bar{W}\left(\begin{array}{c}\text{first-collision neutron source} \\ \text{at } \underline{r}',E',\underline{\Omega}',t')\end{array}\right)}{\Sigma_t(\underline{r}',E')} \quad . \quad (\text{E.4})$$

The scoring in the adjoint calculation for the four types of α events will now be considered (the notation is the same as in Appendix A):

a. **Epithermal Elastic Scattering with an Isotope.**
The first-collision elastic scattering source may
be derived by beginning with an expression for the
first-flight neutron flux at $\underline{r}'',E'',\underline{\Omega}'',t''$, due to a
unit neutron source at $\underline{r},E,\underline{\Omega},t$, as given by[18]

$$
g(\underline{r}'',E'',\underline{\Omega}'',t'';\underline{r},E,\underline{\Omega},t) = \left\{ \frac{e^{-\int_{\underline{r}}^{\underline{r}''} \Sigma_t(s,E)ds}}{|\underline{r}'' - \underline{r}|^2} \delta(\underline{\Omega} - \underline{\Omega}'') \right.
$$

$$
\left. \delta\left[\underline{\Omega}'' - \frac{(\underline{r}'' - \underline{r})}{|\underline{r}'' - \underline{r}|}\right] \delta\left(t'' - t - \frac{|\underline{r}'' - \underline{r}|}{V}\right) \delta(E - E'') \right\} ,
$$

(E.5)

where s denotes an integration along a straight-line
path. If g_θ is defined to be the first-flight neu-
tron flux due to the source S, g_θ may be expressed
as

where

$$
E = \frac{2E'}{(1 - \bar{\alpha})\,\mu_{cm} + 1 + \bar{\alpha}} \tag{E.8}
$$

$$
\mu_{cm} = \left[-1 + \mu_L^2 + \mu_L \sqrt{\mu_L^2 - (1 - A^2)}\right] \Big/ A \quad , \tag{E.9}
$$

$$
\mu_L = -\underline{\Omega} \cdot \underline{\Omega}' \quad , \tag{E.10}
$$

$$
\underline{\Omega} = \frac{\underline{r}' - \underline{r}_\theta}{|\underline{r}' - \underline{r}_\theta|} \quad . \tag{E.11}
$$

Therefore, the contribution that an elastic colli-
sion of the pseudoneutron makes to the estimate J
is given by

$$
g_\theta(\underline{r}'',E'',\underline{\Omega}'',t'';S) = \iiiint g(\underline{r}'',E'',\underline{\Omega}'',t'';\underline{r},E,\underline{\Omega},t)\, S(\underline{r},E,\underline{\Omega},t)d^3\,rdEd\underline{\Omega}dt
$$

$$
= \left\{ \frac{e^{-\int_{\underline{r}_\theta}^{\underline{r}''} \Sigma_t(s,E'')ds}}{|\underline{r}'' - \underline{r}_\theta|^2}\, S_\theta\left(E'',\underline{\Omega}'',t'' - \frac{|\underline{r}'' - \underline{r}_\theta|}{V}\right) \delta\left[\underline{\Omega}'' - \frac{(\underline{r}'' - \underline{r}_\theta)}{|\underline{r}'' - \underline{r}_\theta|}\right] \right\} . \tag{E.6}
$$

The first-collision elastic scattering source at
$\underline{r}',E',-\underline{\Omega}',t'$ is then given by

$$
\iint \left(g_\theta(\underline{r}',E'',\underline{\Omega}'',t';S)\, \Sigma_{s1}^i(\underline{r}',E'')\, \frac{D_1^i(-\underline{\Omega}'' \cdot \underline{\Omega}';\underline{r},E'')_L}{2\pi}\, \delta\left\{E' - \frac{E''[(1 - \bar{\alpha})\mu_{cm} + 1 + \bar{\alpha}]}{2}\right\}_{E'}\, dE''\, d\underline{\Omega}'' \right)
$$

$$
= \frac{e^{-\int_{\underline{r}_\theta}^{\underline{r}'} \Sigma_t(s,E)ds}}{|\underline{r}' - \underline{r}_\theta|^2}\, \frac{S_\theta\left(E,\underline{\Omega},t' - \frac{|\underline{r}' - \underline{r}_\theta|}{V}\right) \Sigma_{s1}^i(\underline{r}',E)D_1^i(\mu_L;\underline{r},E')_L\, E}{2\pi\, E'} \quad , \tag{E.7}
$$

$$J = J' + \frac{\overline{W} * e^{-\int_{r_\theta}^{r'} \Sigma_t(s,E)ds} \, S_\theta\left(E,\underline{\Omega},t' - \frac{|\underline{r}' - \underline{r}_\theta|}{v}\right) \Sigma_{s1}^i(\underline{r}',E) D_1^i(\mu_L;\underline{r},E')_L \, E}{\Sigma_t(\underline{r}',E') 2\pi |\underline{r}' - \underline{r}_\theta|^2 \, \overline{q}_1(j,k,i) \, E'} \quad , \tag{E.12}$$

where

$$D_1^i(\mu_L;\underline{r},E)_L = D_1^i(\mu_{cm};\underline{r},E)_{cm} \frac{d\mu_{cm}}{d\mu_L}$$

$$= D_1^i(\mu_{cm};\underline{r},E)_{cm} \left(2\mu_L + \sqrt{\mu_L^2 - (1 - A^2)} + \frac{\mu_L^2}{\sqrt{\mu_L^2 - (1 - A^2)}}\right) \Big/ A \quad . \tag{E.13}$$

b. _Inelastic Scattering with a Continuum Density Function._ The first-collision source for an event of type 2 is given by

$$\iint_{E_L}^{E_u} g_\theta(\underline{r}',E'',\underline{\Omega}'',t';S) \sum_i \Sigma_2^i(\underline{r}',E'') c_2^i(E',-\underline{\Omega}';\underline{r}',E'',\underline{\Omega}'') dE'' \, d\underline{\Omega}''$$

$$= \int_{E_L}^{E_u} \left[\frac{e^{-\int_{r_\theta}^{r'} \Sigma_t(s,E'')ds}}{|\underline{r}' - r_\theta|^2} S_\theta\left(E'',\underline{\Omega},t' - \frac{|\underline{r}' - \underline{r}_\theta|}{v''}\right) \sum_i \Sigma_2^i(\underline{r}',E'') c_2^i(E',-\underline{\Omega}';\underline{r}',E'',\underline{\Omega}) \, dE'' \right] , \tag{E.14}$$

where

$$\underline{\Omega} = \frac{\underline{r}' - \underline{r}_\theta}{|\underline{r}' - \underline{r}_\theta'|} \quad , \tag{E.15}$$

$$E_L = E' + \sum_{\beta'=1}^{\beta-1} \Delta E_{\beta'} \quad , \tag{E.16}$$

$$E_u = E' + \sum_{\beta'=1}^{\beta} \Delta E_{\beta'} \quad . \tag{E.17}$$

The numerical evaluation of the integral in Eq. (E.14) may be avoided by selecting an energy E from the density function

$$f(E;E') = \frac{1}{E_u - E_L} \quad , \qquad \text{for } E_L \leq E \leq E_u \quad . \tag{E.18}$$

The score is then given by

$$J = J' + \frac{\overline{W}*e^{-\int_{r_\theta}^{r'} \Sigma_t(s,E)ds} \, S_\theta\left(E,\underline{\Omega},t' - \frac{|\underline{r}' - \underline{r}_\theta|}{v}\right) \sum_i \Sigma_2^i(\underline{r}',E)c_2^i(E',-\underline{\Omega}';\underline{r}',E,\underline{\Omega})(E_u - E_L)}{\Sigma_t(\underline{r}',E') \, \overline{q}_2(j,k,\beta)|\underline{r}' - \underline{r}_\theta|^2} \; .$$

<div align="right">(E.19)</div>

This yields the correct expectation value for a collision at $\underline{r}',E',\underline{\Omega}',t'$.

c. Inelastic Scattering with a Discrete Model.

(1) <u>Laboratory system.</u> The first-collision neutron source for this event is given by

$$\iint \left\{ g_\theta(\underline{r}',E'',\underline{\Omega}'',t';S) \, \Sigma_3^i(\underline{r}',E'')_\ell \, \frac{1}{2\pi} D_3^i(-\underline{\Omega}' \cdot \underline{\Omega}'';\underline{r}',E'')_\ell \, \delta\left[E' - \frac{(E''-\epsilon)}{\eta}\right]_{E'} \nu_3^i(\underline{r},E'')_\ell \, dE'' \, d\underline{\Omega}'' \right\}$$

$$= \frac{e^{-\int_{r_\theta}^{r'} \Sigma_t(s,E)ds} \, \Sigma_3^i(\underline{r}',E)_\ell S_\theta\left(E,\underline{\Omega},t' - \frac{|\underline{r}' - \underline{r}_\theta|}{v}\right) \frac{1}{2\pi} D_3^i(\mu_L;\underline{r}',E)_\ell \eta \nu_3^i(\underline{r}',E)_\ell}{|\underline{r}' - \underline{r}_\theta|^2}$$

<div align="right">(E.20)</div>

where

$$\mu_L = -\underline{\Omega}' \cdot \underline{\Omega} \quad , \tag{E.21}$$

$$\underline{\Omega} = \frac{\underline{r}' - \underline{r}_\theta}{|\underline{r}' - \underline{r}_\theta|} \quad , \tag{E.22}$$

$$E = \eta E' + \epsilon \quad . \tag{E.23}$$

The contribution of the collision to the estimate is given by

$$J = J' + \frac{\overline{W}*e^{-\int_{r_\theta}^{r'} \Sigma_t(s,E)ds} \, S_\theta\left(E,\underline{\Omega},t' - \frac{|\underline{r}' - \underline{r}_\theta|}{v}\right) \Sigma_3^i(\underline{r}',E)_\ell D_3^i(\mu_L;r',E)_\ell \eta \nu_3^i(\underline{r}',E)_\ell}{\Sigma_t(\underline{r}',E') \, \overline{q}_3(j,k,i,\ell)|\underline{r}' - \underline{r}_\theta|^2 \, 2\pi} \; . \tag{E.24}$$

(2) <u>Center-of-Mass System.</u>
The first-collision neutron source for this event is given by

$$\iint g_\theta(\underline{r}',E'',\underline{\Omega}'',t';S) \, \Sigma_3^i(\underline{r}',E'')_\ell \, c_3^i(E',-\underline{\Omega}';\underline{r}',E'',\underline{\Omega}'')_\ell \, dE'' \, d\underline{\Omega}''$$

$$= \int \frac{e^{-\int_{r_\theta}^{r'} \Sigma_t(s,E'')ds}}{|\underline{r}' - \underline{r}_\theta|^2} \, S_\theta\left(E'',\underline{\Omega},t' - \frac{|\underline{r}' - \underline{r}_\theta|}{v''}\right) \Sigma_3^i(\underline{r}',E'')_\ell \, c_3^i(E',-\underline{\Omega}';\underline{r}',E'',\underline{\Omega})_\ell \, dE'' \; . \tag{E.25}$$

The integration over E'' may be performed by expanding c_3^i as c_2^i was previously expanded in Eq. (A.23) for

the continuous case. Thus, c_3^i may be expanded as

$$c_3^i(E',-\underline{\Omega}';\underline{r}',E'',\underline{\Omega})_\ell = c_3^i(E'_{cm},\mu_{cm};\underline{r}',E'',\underline{\Omega})|J|$$

$$= \frac{1}{2\pi} c_3^i(\mu_{cm};\underline{r}',E'',\underline{\Omega})_{cm} \delta(E'' - \eta E'_{cm} - \epsilon)_{E'_{cm}} v_3^i(\underline{r}',E'')_\ell |J| \quad , \qquad (E.26)$$

where

$$|J| = \sqrt{\frac{E'}{E'_{cm}}} \quad . \qquad (E.27)$$

The integration over E'' may now be performed to obtain the contribution of the collision to the estimate as

$$J = J' + \left[\frac{\overline{W} e^{-\int_{\underline{r}_\theta}^{\underline{r}'} \Sigma_t(s,E)ds} S_\theta\left(E,\underline{\Omega},t' - \frac{|\underline{r}' - \underline{r}_\theta|}{V}\right) \Sigma_3^i(\underline{r}',E)_\ell D_3^i(\mu_{cm};\underline{r}',E)_{cm} \eta \sqrt{\frac{E'}{E'_{cm}}} v_3^i(\underline{r}',E)_\ell}{\left[\Sigma_t(\underline{r}',E')\overline{Q}_3(j,k,i,\ell) 2\pi|\underline{r}' - \underline{r}_\theta|^2\right]} \right] \qquad (E.28)$$

where

$$\mu_L = -\underline{\Omega} \cdot \underline{\Omega}'$$

$$E = \frac{\left\{ 2\mu_L^2 E' + \left[\frac{(A + 1)^2 - \eta}{\eta}\right]\left[\frac{\epsilon}{\eta} + E'\right] \pm \mu_L \sqrt{4\mu_L^2(E')^2 + \frac{4E'}{\eta}\left[(A + 1)^2 - \eta\right]\left[\frac{\epsilon}{\eta} + E'\right]} \right\}}{\left[\frac{(A + 1)^2 - \eta}{\eta(A + 1)}\right]^2} \quad , \qquad (E.29)$$

$$E'_{cm} = \frac{(E - \epsilon)}{\eta} \qquad (E.30)$$

$$\mu_{cm} = \mu_L \sqrt{\frac{E'}{E'_{cm}}} - \left[\sqrt{\frac{E}{E'_{cm}}}\Big/(A + 1)\right] \quad , \qquad (E.31)$$

for energies such that $E > \epsilon$ and $|\mu_{cm}| < 1$. There is no contribution if E is less than ϵ or $|\mu_{cm}| > 1$.

The solution for E in Eq. (E.29) was obtained by inserting E'_{cm}, as given by Eq. (E.30), into Eq. (A.27), and solving for E. Note that two solutions for E may be obtained, where each solution has $E > \epsilon$ and $|\mu_{cm}| < 1$. If this is the case, the right-hand side of Eq. (E.28) should be written as a sum of the contribution from each E.

d. Fission. The first-collision neutron source for this event is given by

$$\iint g_\theta(\underline{r}',E'',\underline{\Omega}'',t';S) \sum_1 v_4^i(\underline{r}',E'') \Sigma_4^i(\underline{r}',E'') \gamma(E') \frac{1}{4\pi} dE'' d\underline{\Omega}''$$

45

$$= \frac{\int_{(E^L)_{j'}}^{(E^u)_{j'}} e^{-\int_{r_\theta}^{r'} \Sigma_t(s,E'')ds} S_\theta\left(E'',\underline{\Omega},t' - \frac{|r' - r_\theta|}{v}\right) \sum_i v_4^i(\underline{r}',E'') \Sigma_4^i(\underline{r}',E'') \gamma(E'')dE''}{|\underline{r}' - \underline{r}_\theta|^2 \, 4\pi} \quad . \quad (E.32)$$

The evaluation of the integral in Eq. (E.32) may be avoided by selecting the energy E from the density function,

$$F(E;E') = \frac{1}{(E^u)_{j'} - (E^L)_{j'}} \quad , \qquad \text{for } (E^L)_{j'} \leq E \leq (E^u)_{j'} \quad . \quad (E.33)$$

The score is then given by

$$J = J' + \frac{\left\{\overline{W} \, e^{-\int_{r_\theta}^{r'} \Sigma_t(s,E'')ds} S_\theta\left(E,\underline{\Omega},t' - \frac{|r' - r_\theta|}{v}\right) \sum_i v_4^i(\underline{r}',E) \Sigma_4^i(\underline{r}',E) \gamma(E')\left[(E^u)_{j'} - (E^L)_{j'}\right]\right\}}{\left[\Sigma_t(\underline{r}',E')\overline{Q}_4(j,k,j') \, 4\pi \, |r' - r_\theta|^2\right]} \quad .$$

$$(E.34)$$

This gives the correct expectation value for a collision at $\underline{r}',E',\underline{\Omega}',t'$.

2. Derivation of the Scoring Equation for the First Flight of the Pseudoneutron

The results in part 1 do not include the first flight's contribution to the functional. The first-flight contribution to the functional J may be obtained from Eq. (8) as

$$J_f = \iint G^+(\underline{R}';\underline{R}) \, S(\underline{R}') \, \Sigma(\underline{R}) \, d\underline{R}' \, d\underline{R} \quad , \quad (E.35)$$

where G^+ in Eq. (E.35) is obtained as the solution of Eq. (6) with the collision source term omitted; this yields the first-flight contribution. The transformed adjoint Green's function satisfies the same equation as the corresponding Green's function for the transport equation. Therefore, by using the relationship between the transformed adjoint Green's function and the adjoint Green's function of Eq. (11), one may use Eq. (E.5) to express the adjoint Green's function as

$$G^+(\underline{r}',E',\underline{\Omega}',t';\underline{r},E,\underline{\Omega},t) = \frac{e^{-\int_r^{r'} \Sigma_t(s,E)ds}}{|\underline{r}' - \underline{r}|^2} \delta(-\underline{\Omega} + \underline{\Omega}') \delta\left(-\underline{\Omega}' - \frac{(\underline{r}' - \underline{r})}{|\underline{r}' - \underline{r}|}\right) \delta\left(-t' + t - \frac{|\underline{r}' - \underline{r}|}{v}\right) \delta(E - E') \quad .$$

$$(E.36)$$

This expression for G^+ may be inserted into Eq. (E.35), with S given by Eq. (E.1), and the integration may be performed over the $\underline{R}'$ and $\underline{\Omega}$ variables to obtain

$$J_f = \iiint \frac{e^{-\int_{r_\theta}^{r'} \Sigma_t(s,E)ds}}{|\underline{r}' - \underline{r}_\theta|^2} S_\theta\left(E,\underline{\Omega},t - \frac{|\underline{r} - \underline{r}_\theta|}{v}\right)\Sigma(\underline{r}',E,\underline{\Omega},t)d^3r'dEdt \quad , \quad (E.37)$$

where some variable changes $(\underline{r} \Rightarrow \underline{r}')$ and

$$\underline{\Omega} = \frac{\underline{r}' - \underline{r}_\theta}{|\underline{r}' - \underline{r}_\theta|} \quad , \tag{E.38}$$

have been made.

This first-flight contribution may be estimated in the sampling from the adjoint equation by selecting the initial pseudoneutron parameters from a density function $\bar{g}(\underline{r}',E,\underline{\Omega}_a'',t)$, assigning an initial weight of

$$\bar{W} = \frac{\Sigma(\underline{r}',E,-\underline{\Omega}_a'',t)}{\bar{g}(\underline{r}',E,\underline{\Omega}_a'',t)} \quad , \tag{E.39}$$

and computing the contribution to J as

$$J_f = \left[\bar{W} \; S_\theta \left(E,\underline{\Omega},t - \frac{|\underline{r}' - \underline{r}_\theta|}{V} \right) \frac{\bar{g}(\underline{r}',E,\underline{\Omega}_a'',t)}{\int \bar{g}(\underline{r}',E,\underline{\Omega}_a',t)d\underline{\Omega}_a'} \; \frac{\Sigma(\underline{r}',E,\underline{\Omega},t)}{\Sigma(\underline{r}',E,-\underline{\Omega}_a'',t)} \; \frac{e^{-\int_{\underline{r}_\theta}^{\underline{r}'} \Sigma_t(s,E)ds}}{|\underline{r}' - \underline{r}_\theta|^2} \right] \quad . \tag{E.40}$$

The expectation value of J_f in Eq. (E.40) is simply J_f of Eq. (E.37).

3. The Point-Source Estimator Utilized in MCNA

Equations (E.12), (E.19), (E.24), (E.28), (E.34), and (E.40) express the point-source score for the event, or first flight, as a given factor, denoted by ANL in the program, multiplied by the source density $S_\theta(E,\underline{\Omega},t' - |\underline{r}' - \underline{r}_\theta|/V)$. The MCNA program computes the factor ANL*, describes the vector Ω by the cosines $-u$, $-v$, and $-w(\underline{\Omega} = - u\underline{i} - v\underline{j} - w\underline{k})$, sets the variable TME to $t' - |\underline{r}' - \underline{r}_\theta|V$, sets KASR to 3, and calls subroutine SCORE. This procedure is performed for the source pseudoneutron and at each subsequent pseudoneutron collision for each neutron point source.

The point neutron source number for a given call into subroutine SCORE is denoted by the variable IDETX. The general procedure in SCORE is to set

$$\text{TSCOR(IDETX)} = \text{TSCOR(IDETX)} + \text{ANL}^* \text{ (neutron-source density of source IDETX)} \tag{E.41}$$

each time subroutine SCORE is called.

As an example, the following fictitious problem is considered with the two point neutron sources:

---

*For source pseudoneutrons, the factor ANL is computed as

$$\text{ANL} = \frac{\bar{W} \; e^{-\int_{\underline{r}_\theta}^{\underline{r}'} \Sigma_t(s,E)ds}}{4\pi |\underline{r}' - \underline{r}_\theta|^2} \quad .$$

The assumption here is that Σ and $\bar{g}$ in Eq. (E.40) are independent of Ω. If this is not true, the quantity

$$\frac{\bar{g}(\underline{r}',E,\underline{\Omega}_a'',t)}{\int \bar{g}(\underline{r}',E,\underline{\Omega}_a',t)d\underline{\Omega}_a'} \; \frac{\Sigma(\underline{r}',E,\underline{\Omega},t)}{\Sigma(\underline{r}',E,-\underline{\Omega}_a'',t)} \; 4\pi$$

of Eq. (E.40) must be computed in subroutine SCORE and multiplied by ANL.

$\theta = 1$

$$S_1(E,\underline{\Omega},t) = \frac{1}{4\pi} \frac{1}{3 \text{ MeV}} \frac{1}{100} \text{ shakes, for } 1 \text{ MeV} < E < 4 \text{ MeV}$$

$$0 < t < 100 \text{ shakes}$$

$$= 0 \quad \text{otherwise;}$$

$\theta = 2$

$$S_2(E,\underline{\Omega},t) = \frac{1}{4\pi} \frac{1}{5 \text{ MeV}} \frac{1}{1000} \text{ shakes, for } 1 \text{ MeV} < E < 6 \text{ MeV}$$

$$0 < t < 1000 \text{ shakes}$$

$$= 0 \quad \text{otherwise.}$$

Then subroutine SCORE may be written as shown in Fig. E.1.

```
      SUBROUTINE SCORE (KASR)
INTEGER, DIMENSION, COMMON, AND EQUIVALENCE state-
ments corresponding to those of the main program
ATMC.
C     SCORING FOR FICTITIOUS PROBLEM
C     WITH POINT NEUTRON SOURCE
C     ANL = FACTOR TO MULTIPLY BY
C     SOURCE DENSITY
C     -u, -v, -w ARE THE DIRECTION
C     COSINES FROM THE POINT DETECTOR
C     TO THE COLLISION POINT
      IF(KASR.NE.3) GO TO 25
      IF(ERG.LT.1.) GO TO 25
      IF(TME.LT.0.) GO TO 25
      IF(IDETX.GT.1) TO TO 19
      IF(ERG.GT.4.) GO TO 25
      IF(TME.GT.100.) GO TO 25
      TSCOR(1) = TSCOR(1) + ANL/(12.566*300.)
      GO TO 25
19    IF(ERG.GT.6.) GO TO 25
      IF(TME.GT.1000.) GO TO 25
      TSCOR(2) = TSCOR(2) + ANL/(12.566*5000.)
25    RETURN
      END
```

Fig. E.1 Subroutine SCORE for a fictitious problem with two point neutron sources.

APPENDIX F

NEUTRON SOURCES CONTAINING A DELTA FUNCTION IN TIME

An extraneous neutron source, consisting of a pulse in time, presents a problem for scoring in the adjoint calculation because all scoring must be made at a fixed time in the life history of the pseudoneutron. Provided that the functional of interest is not also discrete in the time domain and assuming that the medium is stationary, it is possible to find an equivalent problem that does not involve a discrete neutron source in time.

The nuetron source is assumed to be of the form

$$S(\underline{r},E,\underline{\Omega},t) = S_o(\underline{r},E,\underline{\Omega})\ \delta(t) \quad , \quad (F.1)$$

where $S_o(\underline{r},E,\underline{\Omega})$ is independent of time. The functional of interest is assumed to be given by

$$J = \int_{t_1}^{t_2} \iiint \varphi(\underline{r},E,\underline{\Omega},t)\Sigma(\underline{r},E,\underline{\Omega})d^3r\,dE\,d\underline{\Omega}\,dt \quad , \quad (F.2)$$

where $t_2 > t_1$.

An equivalent problem is now proposed. The geometrical and material characteristics of the original problem remain unchanged in the equivalent problem. The equivalent source is given by

$$S_e(\underline{r},E,\underline{\Omega},t) = \frac{S_o(\underline{r},E,\underline{\Omega})}{\Delta t} \quad \text{for } 0 < t < \Delta t \quad (F.3)$$

$$= 0 \quad \text{otherwise,}$$

where $\Delta t = t_2 - t_1$. Then the equivalent functional is

$$J_e = \iiint \varphi_e(\underline{r}, E, \underline{\Omega}, t_2) \, \Sigma(\underline{r}, E, \underline{\Omega}) d^3 r dE d\underline{\Omega} \Delta t \quad , \quad \text{(F.4)}$$

where φ_e is the neutron flux in the equivalent problem.

The proof that $J_e = J$ is obtained by expressing φ_e in terms of Green's functions and noting that the Green's functions G and G_e are equal for identical arguments; this follows because the geometrical and material characteristics are identical in the two problems. The neutron flux in the two problems may be expressed as

$$\varphi(\underline{r}, E, \underline{\Omega}, t) = \iiiint G(\underline{r}, E, \underline{\Omega}, t; \underline{r}', E', \underline{\Omega}', t') \, S(\underline{r}', E', \underline{\Omega}', t') \, d^3 r' dE' d\underline{\Omega}' dt'$$

$$= \iiint G(\underline{r}, E, \underline{\Omega}, t; \underline{r}', E', \Omega', 0) \, S_o(\underline{r}', E', \underline{\Omega}') \, d^3 r' dE' d\underline{\Omega}' \quad , \quad \text{(F.5)}$$

$$\varphi_e(\underline{r}, E, \underline{\Omega}, t_2) = \int_0^{\Delta t} \iiint G(\underline{r}, E, \underline{\Omega}, t_2; \underline{r}', E', \underline{\Omega}', t') \, \frac{S_o(\underline{r}', E', \underline{\Omega}')}{\Delta t} \, d^3 r' dE' d\underline{\Omega}' dt' \quad , \quad \text{(F.6)}$$

where the expressions for S and S_e in Eqs. (F.1) and (F.3) were used. The equivalence of G and G_e was utilized to obtain the latter expression in Eq. (F.6).

The expressions for the neutron flux in Eqs. (F.5) and (F.6) may be used in Eqs. (F.2) and (F.4), respectively, to obtain

$$J = \int_{t_1}^{t_2} \iiiint \left[G(\underline{r}, E, \underline{\Omega}, t; \underline{r}', E', \Omega', 0) \, S_o(\underline{r}', E', \underline{\Omega}') \, \Sigma(\underline{r}, E, \underline{\Omega}) d^3 r' dE' d\underline{\Omega}' d^3 r dE d\underline{\Omega} dt \right] \quad , \quad \text{(F.7)}$$

$$J_e = \int_0^{\Delta t} \iiiint \left[G(\underline{r}, E, \underline{\Omega}, t_2; \underline{r}', E', \Omega', t') \, \frac{S_o(\underline{r}', E', \underline{\Omega}')}{\Delta t} \, \Sigma(\underline{r}, E, \underline{\Omega}) \Delta t d^3 r' dE' d\underline{\Omega}' d^3 r dE d\underline{\Omega} dt' \right] \quad . \quad \text{(F.8)}$$

In Eq. (F.8) the change of variables,

$$t = (t_2 - t') \quad , \quad \text{(F.9)}$$

is now made to obtain

$$J_e = \int_{t_1}^{t_2} \iiiint \left[G(\underline{r}, E, \underline{\Omega}, t; \underline{r}', E', \underline{\Omega}', 0) S_o(\underline{r}', E', \underline{\Omega}') \, \Sigma(r, E, \underline{\Omega}) d^3 r' dE' d\underline{\Omega}' d^3 r dE d\underline{\Omega} dt \right] \quad , \quad \text{(F.10)}$$

where a stationary system has been assumed so that

$$G(\underline{r}, E, \underline{\Omega}, t_2; \underline{r}', E', \underline{\Omega}', t_2 - t)$$

$$= G(\underline{r}, E, \underline{\Omega}, t; \underline{r}', E', \underline{\Omega}', 0) \quad . \quad \text{(F.11)}$$

The right-hand sides of Eqs. (F.7) and (F.10) are identical, which proves that $J = J_e$ as postulated. Therefore, the reciprocity relationship may be substituted into Eq. (F.8) to evaluate the functional, by sampling from the adjoint equation, as

$$J = \int_0^{\Delta t} \iiiiint \left[G^+(\underline{r}', E', \underline{\Omega}', t'; \underline{r}, E, \underline{\Omega}, t_2) \right.$$

$$\left. \frac{S_o(r', E', \underline{\Omega}')}{\Delta t} \, \Sigma(\underline{r}, E, \underline{\Omega}) \Delta t d^3 r' dE' d\underline{\Omega}' d^3 r dE d\underline{\Omega} dt' \right] \quad .$$

$$\text{(F.12)}$$

Therefore, in the sampling from the adjoint equation, the initial time is set to t_2, the remaining initial coordinates of the pseudoneutron may be selected with the density function

$$\bar{g}(\underline{r},E,\underline{\Omega}_a) = \frac{1}{4\pi} g(E) \frac{1}{V} \quad , \qquad (F.13)$$

for $\underline{r}$ in the volume V containing nonzero Σ, and the initial weight may be set to

$$\bar{W} = \frac{\Sigma(\underline{r},E,-\underline{\Omega}_a)}{\bar{g}(r,E,\underline{\Omega}_a)} \quad . \qquad (F.14)$$

Here an isotropic selection of the direction of flight and a uniform selection of the position have been specified for illustration.

If a volumetric source is assumed (i.e., not a surface source), the score at each collision is obtained from Eq. (36) as

$$\frac{\bar{W} * S_o(\underline{r},E,-\underline{\Omega}_a)}{\Sigma_t(\underline{r},E)} \quad , \qquad (F.15)$$

whenever $0 < t < \Delta t$.

This derivation is valid under the assumptions that: (1) the system is not changing with time, and (2) the scoring cross section Σ is independent of time.

REFERENCES

1. J. M. Hammersley and D. C. Handscomb, Monte Carlo Methods, John Wiley & Sons, New York, 1964.

2. L. L. Carter, unpublished University of Washington Ph.D. dissertation (1969).

3. L. L. Carter and N. J. McCormick, Nucl. Sci. Eng., 39, 296 (1970).

4. Description of the MCN Computer Code; to be published.

5. R. R. Johnston, "A General Monte Carlo Neutronics Code," Los Alamos Scientific Laboratory report LAMS-2856 (1963).

6. W. M. Taylor, "MCH User's Guide," Los Alamos Scientific Laboratory internal document, 1968. (SECRET)

7. A. M. Weinberg and E. P. Wigner, The Physical Theory of Neutron Chain Reactors, University of Chicago Press, Chicago, 1958.

8. J. Lewins, Importance: The Adjoint Function, Pergamon Press, London 1965.

9. G. Goertzel and M. H. Kalos, "Monte Carlo Methods in Transport Problems," Progress in Nuclear Energy, Series 1, Vol. 2, Pergamon Press, New York, 1958.

10. J. Spanier and E. M. Gelbard, Monte Carlo Principles and Neutron Transport Problems, Addison-Wesley Publishing Company, Reading, Massachusetts, 1969.

11. A. E. Profio, Editor, "Shielding Benchmark Problems," Oak Ridge National Laboratory report ORNL-RSIC-25 (1969), pages 3.0-1 to 3.0-31.

12. L. L. Carter, Trans. Am. Nucl. Soc. 12, 2, 730 (1969).

13. Private Communication.

14. M. M. R. Williams, The Slowing Down and Thermalization of Neutrons, John Wiley and Sons, New York, 1966.

15. F. B. Hildebrand, Advanced Calculus for Engineers, Prentice-Hall, Englewood Cliffs, New Jersey, 1948.

16. M. H. Kalos, Bo Eriksson, Claes Johansson, and Martin Leimdorfer, Nucl. Sci. Eng. 37, 410 (1969).

17. Z. W. Birnbaum, Introduction to Probability and Mathematical Statistics, Harper and Brothers, New York, 1962.

18. A. A. Aswad and G. R. Dalton, Nucl. Sci. Eng. 24, 49 (1966).